# Kent Academic Repository

**Page, Jonathan James (2017)** *Understanding insulin signalling and its role in regulating ageing in C elegans using pharmacological and genetic approaches.* **Master of Science by Research (MScRes) thesis, University of Kent,.**

## Downloaded from

## The version of record is available from

## This document version
UNSPECIFIED

## DOI for this version

## Licence for this version
UNSPECIFIED

## Additional information

## Versions of research works

### Versions of Record

### Author Accepted Manuscripts

## Enquiries

# Understanding insulin signalling and its role in regulating ageing in *C. elegans* using pharmacological and genetic approaches.

MSc by Research
Biochemistry

Jonathan James Page

August 2017

University of Kent
School of Biosciences

Supervisors:
Dr Jennifer Tullet, Professor Michelle Garrett

## Acknowledgments

I would like to thank my supervisors, Dr Jennifer Tullet and Professor Michelle Garrett for providing me with this project and offering assistance and support throughout.

My thanks also go to Max, Dan and Abigail for assistance with *C. elegans* and general support in the lab.

And thanks to Jasmine, Nathan, Edith, Helen, Sarah and Andrew in Michelle Garrett's lab for assistance with the drug aspect of the project.

And finally, gratitude goes to Dr Ian Brown and to Matt Badham for providing guidance in fluorescence microscopy.

# Abstract

Throughout history aging is an impasse humans have aspired to overcome. In *Caenorhabditis elegans*, downregulation of Insulin/IGF-1-like signalling (IIS) through mutation of *daf-2* (equivalent of the human Insulin receptor) has been observed to cause a substantial lifespan extension via AKT1&2, through activation of the transcription factor DAF-16 (human FOXO3A). Many cancer treatment drugs target AKT; I set out to test whether they could be re-purposed as an anti-ageing therapy. Using a DAF-16::GFP overexpressing strain of *C. elegans*, we monitored the IIS pathway in response to competitive and allosteric AKT inhibitors, AT13148 and MK2206 respectively, by examining the degree of DAF-16 nuclear accumulation. AT1341 and MK2206 were found not to induce DAF-16 nuclear localisation at concentrations up to 500μM and 200μM respectively.

Secondly, in a separate but related project I undertook work to explore the activation and functional role of a second transcription factor SKN-1 (human NFE2-related factor), in response to reduced IIS. In particular, an isoform of this transcription factor SKN- 1B, expressed in ASI neurones, remains relatively uncharacterised. Using worms expressing a SKN-1B::GFP transgene, the effect of temperature on SKN-1B::GFP expression in the ASIs in response to reduced IIS was determined. Maintenance of SKN-1B in the neurones was found to require insulin signalling at 20°C and 25°C but not 15°C, this effect involved DAF-16 at 20°C but not 25°C.

Finally, in an effort to understand why skn-1b is required for dietary restriction induced longevity, I explored the role of *skn-1b* in chemo-sensation of food in worms as a function of age. Interestingly, *skn-1b* knockout worms showed reduced foraging behaviour compared to WT under some conditions.

# Contents

# Abbreviations

| | |
|---|---|
| μl | Microlitre |
| 14-3-3 proteins | PAR-5 & FTT-2 |
| A, C, G, T | Adenine, cytosine, guanine, thymine |
| ADP | Adenosine diphosphate |
| AKT | Protein kinase B |
| AMP | Adenosine monophosphate |
| AMPK | 5' adenosine monophosphate-activated protein kinase |
| ANOVA | Analysis of varience |
| ATP | Adenosine triphosphate |
| BR | Basic region |
| BUS | Bacterially unswollen |
| bZIP | Basic leucine zipper |
| $CaCl_2$ | Calcium chloride |
| CaMKII | Ca2+/calmodulin-dependent protein kinase II |
| cDNA | Complementary deoxyribonucleic acid |
| *C. elegans* | *Caenorhabditis elegans* |
| CNC | Cap 'n' collar |
| DAF | Dauer formation |
| DMSO | Dimethyl sulfoxide |
| DNA | Deoxyribonucleic acid |
| DR | Dietary restriction |
| EDTA | Ethylenediaminetetraacetic acid |
| $FeSO_4$ | Iron(II) sulphate |
| FOXO | Forkhead box O |
| FUDR | 5-Fluoro-2'-deoxyuridine |
| GFP | Green fluorescent protein |
| HD | Homeodomain |
| HSP | Heat shock protein |

| | |
|---|---|
| IGF-1 | Insulin-like growth factor 1 |
| IIS | Insulin/insulin-like growth factor signalling |
| JNK | c-Jun N-terminal kinase |
| $KH_2PO_4$ | Monobasic potassium phosphate |
| L1, L2, L3, L4 | 1st, 2nd, 3rd and 4th worm larval stages |
| LB | Lysogeny broth |
| M | Molar |
| mM | Millimolar |
| $MgSO_4$ | Magnesium sulphate |
| $MnCL_2$ | Manganese(II) chloride |
| mRNA | Messenger ribonucleic acid |
| NaCl | Sodium chloride |
| NaOH | Sodium hydroxide |
| NGM | Nematode growth media |
| NMR | Nuclear magnetic resonance |
| Nrf2 | NFE2-related factor 2 |
| OD | Optical density |
| PH | Pleckstrin homology |
| pH | Potential of hydrogen |
| qPCR | Real-time polymerase chain reaction |
| qRT-PCR | Real-time reverse transcription polymerase chain reaction |
| rIIS | Reduced insulin/insulin-like growth factor signalling |
| RNAi | Ribonucleic acid interference |
| ROS | Reactive oxygen species |
| SKN-1 | Skinhead-1 |
| UNC | Uncoordinated |

# 1. Introduction

## *C. elegans* background

The nematode *Caenorhabditis elegans* (*C. elegans*) provides an ideal preliminary model for genetic studies relating to humans. Many pathways are conserved between *C. elegans* and humans, 60-80% of human genes having orthologues in *C. elegans*[1]. Unlike many animals, *C. elegans* is easy and cheap to maintain, living off bacterial cultures in the lab. The short lifespan, up to a month, allows for experiments involving lifespan or crossing several generations of offspring to be conducted within a viable timeframe. The transparent body provides the option of observing cellular activity, for example GFP expression patterns, *in vivo*. In addition, being androdioecious with a low male tendency of ~0.1% of the population[2], clonal descent overwhelms. However strain crosses remain possible through sexual mating; male tendency within the population can be increased by heat shocking L4 worms at 30 Celsius for 5 hours[3] making this process feasible. While in humans, male phenotype arises from presence of a Y-chromosome, in *C. elegans* it is the reduction in ratio of X:Autosome[4], resulting from spontaneous X non-disjunction, which is the determinant.

*C. elegans* goes through several stages during its early life. Embryogenesis lasts ~150 minutes within the parent until the embryo amasses 30 cells and the egg is laid; embryogenesis continues for another 650-700 minutes to which the worm hatches at 588 cells in mass[5]. If sufficient food is present, the new stage-1 larva (L1) continue development; if food is lacking, development arrests and worms may survive for up to 10 days[6]. At the end of each larval stage the outermost layer, the cuticle, is shed and replaced with one chemically and structurally different according to the particular stage advancement[5]. In normal conditions, four moults are required to progress to a fertile adult. If however, conditions become unfavourable e.g. scarce food, high temperature or toxic substances, L1's and L2's may enter an alternative L3 stage called dauer, whereby cuticle morphogenesis occurs and transcription, metabolism and food intake[7][8][9] are reduced, but HSP90[10][11], superoxide dismutase[12] and catalase[13] mRNA's are increased. These changes allow for dauer larvae to endure through harsh conditions for a time period far in excess of the normal lifespan, up to several months.

## Insulin/insulin like growth factor signalling

One of the major effectors in the initiation of dauer is the Insulin/IGF-1-like signalling (IIS) pathway [Figure 1], which bears high similarity to the insulin pathway in humans, with many of the components being commonly derived and showing significant sequence similarity. While it is very important for dauer formation, alterations in the IIS pathway can also lead to increased lifespan, stress resistance and improved late life health including a reduction in age-related degeneration in adult worms[14]. Decreasing DAF-2 (orthologue of the insulin receptor) signalling via mutation in the *daf-2* gene, has been shown to more than double normal lifespan in otherwise wild-type worms, along with reducing ß-amyloid toxicity, associated with the development of Alzheimer's, in transgenic worms[15]. This effect is only observed with functional DAF-16[16] (orthologue to the FOXO transcription factors); it is known that DAF-16 is involved heavily in the signal transduction of the IIS pathway but also functions as a transducer for other signals, including from JNK1 upon exposure to heat stress[17] and UNC-43 (CaMKII) [18]. DAF-16 is a transcription factor, binding to the consensus "TTGTTTAC"[19], its function depending on its localisation within the nucleus, which is regulated via phosphorylation of specific residues. While phosphorylation of DAF-16 by JNK1[17] and CaMKII[18] lead to activation of DAF-16 and its entry into the nucleus, phosphorylation by AKT-1 or AKT-2 of the IIS pathway retains DAF-16 in the cytosol through association with 14-3-3 proteins (PAR-5 and FTT-2) [20][Figure 1]. One direct transcriptional target of DAF-16 is that of the regulatory gamma subunit of AMPK, involved in maintenance of energy levels[21]. However DAF-16 appears to also function as a regulator of other transcription factors, for example transcribing *mdl-1,* encoding the MAD-Like transcription factor[22].
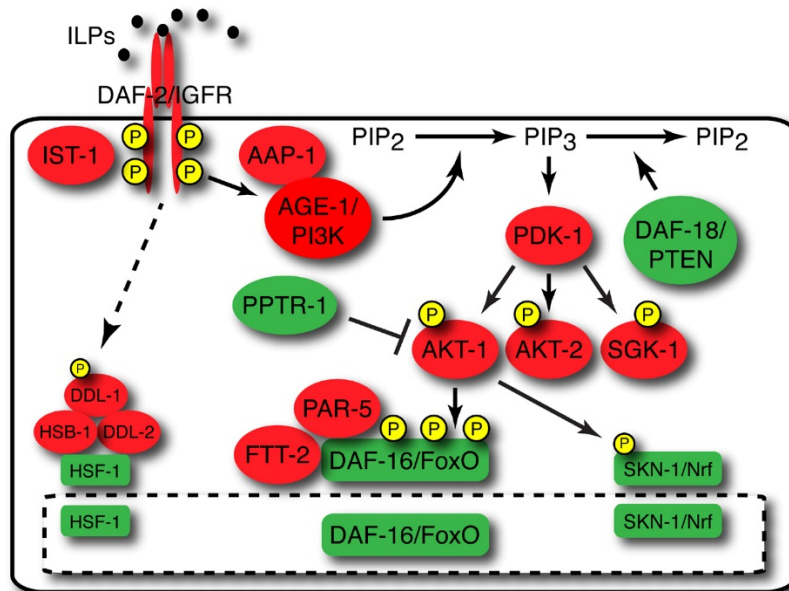
*Figure 1 **Summary figure of IIS signalling pathway.** Figure taken from WormBook[23] Activation of DAF-2 leads to activation of AKT-1, which inhibits DAF-16 and SKN-1 entry to the nucleus by means of phosphorylation.*

## Targeting the IIS pharmacologically

Several drugs have been shown to target various components of the IIS pathway[24],[25], [26]. Provided by our collaborator (Professor M.D.Garrett, University of Kent),

MK-2206 and AT13148 are currently in clinical trials as potential anti-cancer drugs that target AKT.

Current methods for reducing IIS in worms involves genetic manipulation. This would not be an ideal situation in humans. Imitating the effect pharmaceutically to increase longevity is a much more appealing scenario.

MK-2206 binds allosterically to the PH (pleckstrin-homology) domain of AKT[27], inhibiting phosphorylation activity. Another drug, AT13148 in contrast competes with ATP at the ATP binding region[25]. In *C. elegans* this comprises a glycine rich loop: residues 199-207 (LGKGTFGKV)[28]; several residues forming polar interactions: K222, Q271, A273, E277, K318, E320, A333 and two residues involved in hydrophobic interactions: V207, as part of the glycine loop and M323[29] (residue numbers from the canonical sequence of AKT-1.

## Testing drugs in *C. elegans*

In theory worms are a good model to test the effects of drugs on animal health and identify the underlying signalling pathways that they target. However, since direct

injection of drugs is not viable, drugs are delivered to worms mixed with their bacterial food source. Problems arise as drugs are often biotransformed in the bacteria and in addition, do not absorb well through the worms' cuticle[30], thus wild-type *C. elegans* largely resists uptake of drugs. Determining the actual effective concentration of drug is therefore very difficult as this could be much less than that administered. Several attempts have been made to improve drug delivery in nematodes; the most effective appears to be to delivery in liquid media[31] to *bus-8* mutants. *bus-8* encodes a glycosyltransferase (BUS-8), required during embryogenesis for epidermal migration and enclosure; defects of which can result in rupture of the epidermis and consequently are lethal[32]. "Weaker" defects in *bus-8*, such as variant *bus-8(e2885)*[33]*,* are not lethal during embryogenesis, but fail to organise the epidermis and cuticle effectively during the worm larval stages. As a result, the skin becomes less resistant to small molecule permeation and consequently worms are hypersensitive to drugs, permitting lower concentrations to be administered[34] and reducing the potential for stress induced responses from over-administration. In addition, liquid medium allows for the use of 96-well plates with reduced volume compared to conventional agar plates and further reduces the drug quantity used.

## SKN-1

Like DAF-16, the transcription factor SKN-1 also functions as part of the IIS pathway [Figure 1], acting in response to oxidative stress. SKN-1 is the orthologue of the human NFE2-related factor (Nrf2) basic leucine zipper (bZIP) transcription factor, which promotes expression of phase 2 reactive oxygen species (ROS) detoxification enzymes[35]. In *C. elegans*, maternal SKN-1 is required for embryonic endoderm and mesoderm development along with responding to oxidative stress[36] [37]. SKN-1 has retained a variant of the Cap 'n' Collar (CNC) domain but unlike Nrf2 and other conventional bZIP proteins, SKN-1 lacks the ZIP domain that establishes dimerization usually required for DNA binding [Figure 2]. Instead SKN-1 has omitted this step, functioning as a monomer. DNA binding therefore involves a different mechanism than Nrf2 and other bZIP proteins. Along with a conserved basic region (BR) at the carboxyl terminal, SKN-1 possesses a module not shared among Nrf proteins, but shows close homology to the flexible arm of homeodomain proteins (HD arm), which is expressed at the amino terminal of the DNA binding domain. Both the BR and HD arm are essential

for SKN-1 DNA binding, respectively binding the major groove at the bZIP-half site and an AT-rich region of the minor groove.[38] Other than the DNA binding region, little is conserved between SKN-1 and Nrf. However, despite this divergence in the DNA binding mechanism and limited homology, SKN-1 regulates many of the same genes and remains functionally well conserved to its mammalian orthologues, providing an apposite model for the study of Nrf regulation and involvement in ageing[35].

Other than some of the DNA binding elements, one other motif shows high conservation between all Nrf proteins including SKN-1, called DIDLID (SKN-1: EDIDLIDVLWRSDI) [Figure 2]. This region is required for SKN-1 transcription activation and also proteasome degradation via association to the WDR-23 proteins[37].

Oxidative damage is considered as one of the contributing factors in aging, so agents that reduce damage by reactive oxygen species (ROS), such as SKN-1, are looked on favourably for determining longevity[39]. Previous work in *C. elegans* has shown that knockdown of SKN-1, like DAF-16, is detrimental to the long lifespan of worms with reduced insulin/IGF-1 like signalling (rIIS)[40]. Overexpression of SKN-1 has also been shown to increase lifespan without the requirement for rIIS[35]. Recent work however, has identified that the mechanisms behind SKN-1 induced longevity and stress response can be separated [41]. In addition, upregulation of other enzymes tasked with neutralising ROS, not under control of SKN-1, would largely compensate in worms under low stress in a laboratory[39] and so SKN-1 induced longevity is likely to function independently of ROS scavenging.

There are 4 isoforms of *skn-1* [Figure 2], most research has been done with isoform *c*, which is expressed in intestine. One of the four isoforms of *skn-1*, isoform *b* is less well characterised and is predominantly expressed in the ASI chemosensory neurones[42]. SKN-1B lacks the domains required for transcription and the DIDLID motif but possess an exon unique to *skn-1b* with no related sequence among any organism [Figure 2].

**2.1**

SKN-1

Nrf

HD arm

DIDLID    CNC    BR    ZIP

**2.2**

skn-1a

skn-1b

skn-1c

skn-1d

skn-1b
(tm4241)
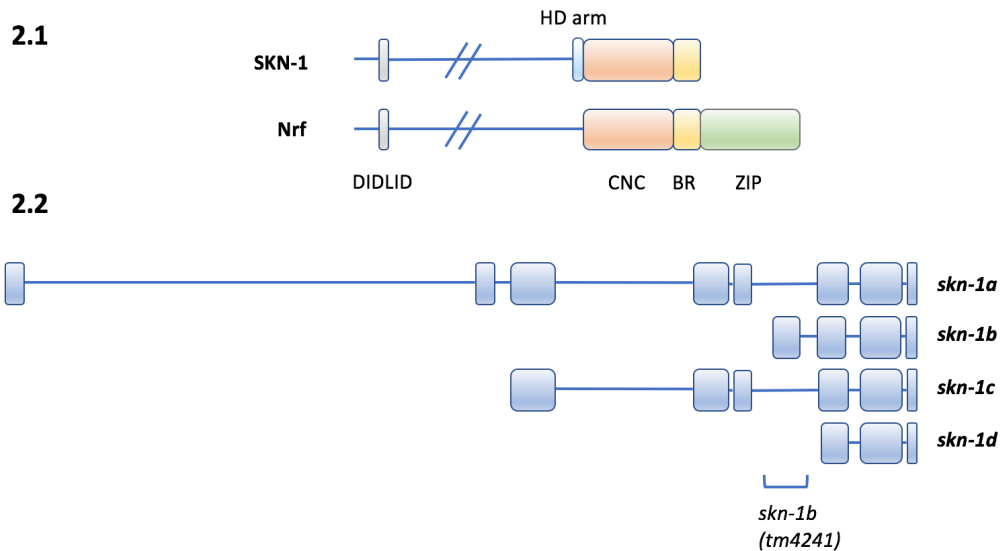
*Figure 2 **The Nrf orthologue in C. elegans, SKN-1, has 4 isoforms.** 2.1) SKN-1 lacks the ZIP domain required form dimerization but possesses a structure analogous to the HD arm of homeodomain proteins. The DIDLID m otif is well conserved between SKN-1 and Nrf. **2.2)** skn-1 has 4 isoforms. skn-1b lacks many of the exons of skn-1a and skn-1c but has an exon unique in sequence to skn-1b. The tm4241 mutation knocks out most of this skn-1b exon. Adapted from figure by T. Keith Blackwell et al 2015*[35]

Along with rIIS in worms, dietary restriction (DR), where nutrient intake is carefully controlled without causing malnutrition, promotes significant lifespan extension in all animals trialled, including *C. elegans*[43]. In worms, the most common method of imposing DR is a reduction in the bacterial food source, usually through bacterial dilution or restricting feeding, such is the case with *eat* mutants which have defects in pharyngeal function[44]. *skn-1* is required for the lifespan extension seen in worms subjected to DR, as knockout of *skn-1* is detrimental to this longevity. Of all 4 isoforms of SKN-1, only rescue of SKN-1B expression in the ASI neurones has been shown to recover this *skn-1* dependant, DR mediated longevity[42].

## Aims of project

This project had three main aims:

**Aim 1)** To determine the effects the anti-cancer drugs, AT13148 and Mk2206, on *C. elegans*; with the view to determine whether they could be used to promote longevity and late life health.

**Aim 2)** Investigate whether SKN-1B expression levels are regulated by the insulin/insulin-like signalling (IIS) pathway.

**Aim 3)** Explore the role of SKN-1B in regulating *C. elegans* feeding behaviours.

# 2. Materials and methods

## 2.1.1. *C. elegans* strains

i.   N2 CGC male population wild type

ii.  JMT10 *bus-8(e2885)* [daf-16::GFP; rol-6,]

iii. TJ356 [daf-16::GFP; rol-6]

iv.  GA1017 [Pskn-1b::skn-1b::GFP]

v.   GA1030 *daf-2 (e1370)*[Pskn-1b::skn-1b::GFP;]

vi.  GA1043 *daf-2(e1370); daf-16(mgDf50)* [Pskn-1b::skn-1b::GFP;]

vii. GA1058 *skn-1b(tm4241)*

Strains: i. and iii. acquired from the Caenorhabditis genetics centre.
Strain: ii. produced in lab.
Strains: iv., v., vi. and vii. acquired from David Gems, University College, London.

## 2.2.1. Nematode Growth Medium (NGM)

*C. elegans* strains were maintained on NGM containing: 3g/l NaCl, 17g/l agar, 2.5g/l peptone, 25mM $KH_2PO_4$ (pH 6), 1mM $MgSO_4$, 1mM $CaCl_2$, 1ml/l of 5mg/ml cholesterol (in ethanol). Worms were fed with viable OP50 strain of *E. coli* grown on NGM plates and maintained at 20°C unless otherwise indicated.

## 2.2.2. Lysogeny broth (LB)

Lysogeny broth (LB) contains: 25g/l Fisher Scientific LB Broth (Miller).

## 2.2.3. Bleach solution

7 parts household bleach to 8 parts 4M NaOH.

## 2.3.1. S-basal

5.9g/l NaCl, 50mM $K_2PO_4$ (pH 6), 1ml/l of 5mg/ml cholesterol in ethanol.
Autoclaved.

## 2.3.2. Trace metals solution

1.86g/l disodium EDTA, 0.69g/l $FeSO_4 \bullet 7H_2O$, 0.2g/l $MnCl_2 \bullet 4H_2O$, 0.29g/l $ZnSO_4 \bullet 7H_2O$, 0.025g/l $CuSO_4 \bullet 5H_2O$. Autoclaved and stored in darkness.

## 2.3.3. S-medium

1l S-basal, 10mM potassium citrate (pH 6) (autoclaved), 10ml trace metals solution, 3mM $CaCl_2$, 3mM $MgSO_4$. Made in sterile conditions within laminar flow cupboard.

## 2.3.4. DMSO toxicity assay

To determine the concentration at which DMSO does not induce nuclear localisation of DAF-16, 15 L4 stage worms were incubated for 24 hours at 20°C in each well of a 96 well plate containing: 88μl S-medium, 2μl of 10 times concentrate of an overnight OP50 culture, 10μl DMSO in $H_2O$ (DMSO: 100%, 50%, 10% 5%, 0%) to give final DMSO concentrations of: 10%, 5%, 1%, 0.5% and 0%, per well. Worms were Imaged by fluorescent microscopy (2.2.3).

## 2.3.5. Drug induced DAF-16 nuclear localisation assay

40 L4 stage worms were incubated for 24 hours at 20 centigrade in each well of a 96 well plate containing: 94.5μl S-medium, 3μl of 10 times concentrate of overnight OP50 culture, 2.5μl of AT13148 in DMSO (stock: 20mM, 12mM, 4mM, 0mM) or $H_2O$. For MK2206, 1μl of drug was used (stock: 20mM, 10mM) with S-medium adjusted to a total volume of 100μl. Worms removed from wells with a glass pipette and allowed to dry for 10 minutes on NGM. Worms were Imaged by fluorescent microscopy (2.3.6). The level of nuclear localisation of GFP-labelled DAF-16 was scored as "low" (dispersed), "medium" (moderate localisation across the worm or strong in few regions) or "high" (complete nuclear localisation across worm) for individual worms; worms displaying no reaction to light mechanical force and showing no pharyngeal pumping were included in results, classed as dead, so long as no obvious natural cause of death was attributed. Data was analysed by Kruskal-Wallis analysis, followed by Dunnetts post hoc if Kruskal-Wallis identified a

significant difference in data between conditions. Following Dunnetts test: * represents $\geq$ 95% confidence that any variation in data in relation to the control was not due to chance and so the null hypothesis, that the two sets of data are the same, was rejected; ** represents $\geq$ 99% confidence.

## 2.3.6. Fluorescent microscopy

Worms were placed into 0.06% tetramisole hydrochloride (made with M9 buffer) on 2% agarose pad (made with M9 buffer) on a microscope slide with coverslip. The worms were imaged with a Leica DMR fluorescent microscope

## 2.3.7. Bacterial growth assay

A fresh OP50 (*E. coli*) culture was grown to $OD_{600}$ of 0.2 in LB and diluted to 1 in 975. 97.5µl was added to each well of a 96 well plate (to give cell number of $1.6 \times 10^4$ per well) and made up to 100µl with drug in DMSO (AT13148 stocks: 20mM, 10mM, 2mM, 200µM, 20µM, 2µM; MK2206 stocks: 20mM, 12mM, 8mM, 4mM, 2mM, 200µM, 20µM, 2µM) so total DMSO concentration was 2.5%; wells with only LB (blank), only water (water), LB + DMSO + OP50 (DMSO) or LB + $H_2O$ + OP50 (untreated), were also made. The plate was sealed with laboratory film and read at $OD_{600}$ by a BMG LABTECH SPECTROstar *Nano* microplate reader, for 25 hours at 25°C. The data was analysed in Microsoft Excel.

## 2.4.1. 5-Fluoro-2'-deoxyuridine (FUDR) plates

Standard 15ml (50mm diameter) NGM plates seeded with 200µl of a bacterial overnight culture and allowed to grow on the plate for 48 hours. 100µl of a 1.5mM solution of FUDR was added to the centre of the bacterial lawn and allowed 24 hours to diffuse.

## 2.4.2. Food avoidance assay

Strains: N2 and GA1058 (*skn-1b*) were bleach synchronised and allowed to grow to L4 stage. The worms were transferred to FUDR plates with 200µl of either an OP50

or HT115 bacterial lawn at the centre of the plate creating a lawn to around one third the diameter of the plate. After several hours, the number of worms on and off the lawn were counted. Counting was repeated for days 1, 2 and 3 and continued to day 10 ad libitum. Paralysed or dead worms were removed.

### 2.5.1. Neuronal SKN-1B::GFP expression quantification

L4 stage worms from strains: GA1017, GA1030, GA1043 from stocks maintained at 15°C, were grown at 15°C, 20°C or 25°C for 24 hours and imaged by fluorescent microscopy (2.3.6) at 400x zoom with an exposure of 3000ms. Neurone fluorescence was quantified in Fiji (imagej) by tracing the neurone and recording mean fluorescence.

# 3. Results

## 3.1. In silico analysis of conservation between *C. elegans* and human AKT-1/AKT1

Because the drugs in question were created for use in mammalian systems we wanted to confirm that they could be effective against worm forms of AKT.

### 3.1.1. The AKT inhibitor AT13148 is likely to interact with *C. elegans* AKT-1

In Mammalia, AT13148 competes with ATP at the ATP binding region [24]. In *C. elegans* this binding region comprises a glycine rich loop: residues 199-207 (LGKGTFGKV) [25]; several residues forming polar interactions: K222, Q271, A273, E277, K318, E320, A333 and two residues involved in hydrophobic interactions: V207, as part of the glycine loop and M323[26] (residue numbers from the canonical sequence of AKT1[25]). This region shows high sequence similarity between all isoforms of AKT1 and AKT2, between Humans and *C. elegans*, which suggests that similar interactions can occur in both species. The crystal structure of a *Homo sapiens-Bos Taurus* chimera of AKT with AT13148 bound shows that many

of these residues involved in the interaction with ATP are required for binding AT13148. To examine how this might interact in worms would require a structure of *C. elegans* AKT-1. Unfortunately no structure was available, so the web program Phyre2 was used to generate one from the canonical sequence for *C. elegans* AKT1 acquired from Uniprot [28]. Phyre2 queries this sequence against the HHBlits database [45] and creates a multiple sequence alignment. The multiple sequence alignment is used to predict secondary structures with PSIPRED [46]; together with the alignment, these are then used to generate a hidden Markov model for the protein. The hidden Markov model is then queried against a database of known structures and initial protein backbone structures are generated. Indels are corrected using a library of protein fragment structures. Phyre2 then uses Poing [47] and Pulchra [48] to create a complete query model, from the separate template generated regions/domains correcting for distance restraints and steric clashes. Finally, side chains are added from a library of residue rotamers to an accuracy of ~80% [49]. The generated AKT1 structure for *C. elegans* was then overlaid on the AT13148 binding structure in Pymol using the align tool. This generates a sequence alignment of all residues between the two sequences and superposition's one model over the other [Figure 3]. This comparison shows that along with the high sequence similarity [Figure 4], the binding site is well preserved, suggesting that *C. elegans* AKT1 (and by extension, likely AKT2) will function similarly in binding AT13148.
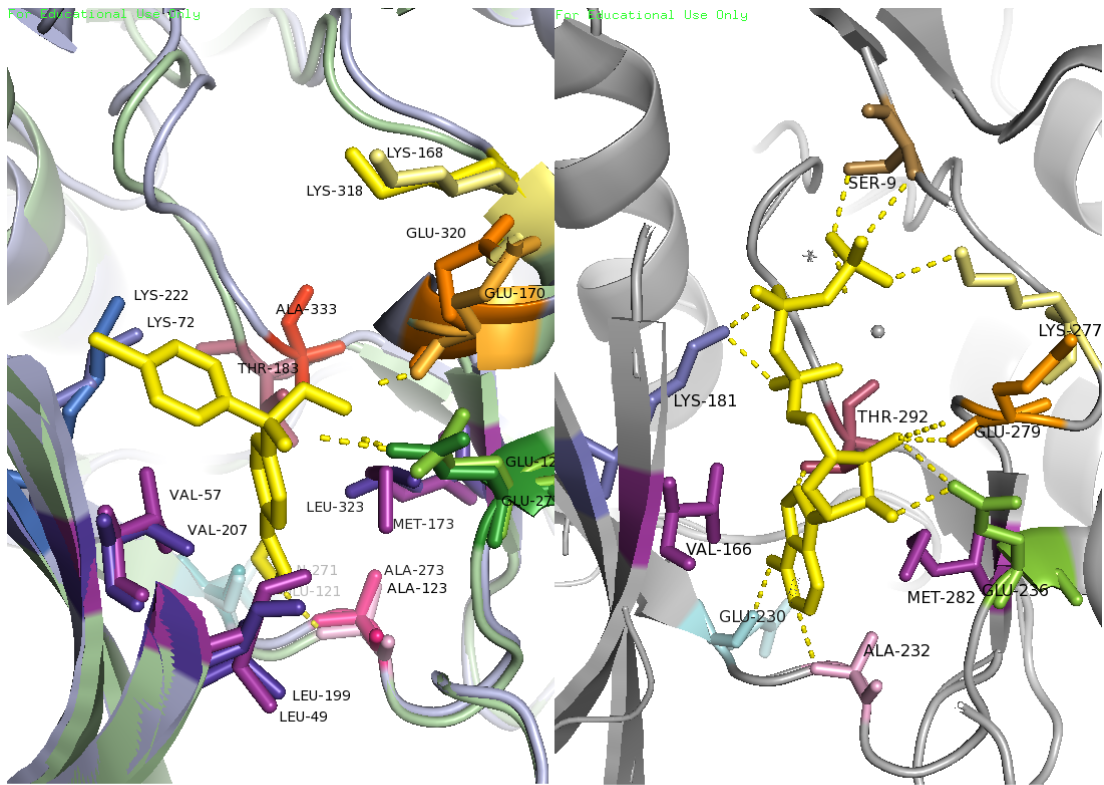
Figure-3.1                                        Figure-3.2

*Figure 3* **The residues and structure for binding AT13148 are well conserved between C. elegans AKT-1 and a mock-up human AKT1.** *Many of the ATP binding residues (**3.2**) are required for AT13148 binding (**3.1**). Comparison of AT13148 binding (figure-3.1, centre yellow) and ANP (ATP analogue) (figure-3.2, centre yellow) at the ATP binding site of AKT. Figure-3.1, AT13148 is bound to a Bos Taurus-Homo sapiens chimera crystal structure (green chain and light coloured residues) (PDB: 4AXA) and overlain with all backbone atoms of a Phyre2 predicted structure for C. elegans AKT1(blue chain and dark coloured residues) (canonical sequence). Figure-3.2, ANP is bound to a Homo sapiens chimera crystal structure (PDB: 1O6L). Residues are colour co-ordinated between figures 3.1 and 3.2. Purple residues are hydrophobic.*

```
C. elegans AKT-1      ADTSEAAKRDKITMEDFDFLKVLGKGTFGKVILCKEKRTQKLYAIKILKKDVIIAREEVA 236
(PDB: 4AXA) AKT1      LKKWENPAQNTAHLDQFERIKTLGTGSFGRVMLVKHMETGNHYAMKILDKQKVVKLKQIE 87
(PDB: 1O6L) AKT1      ----------KVTMNDFDYLKLLGKGTFGKVILVREKATGRYYAMKILRKEVIIAKDEVA 50
                         .    :::*: :* **.*:**:*:* :.   *  . **:*** *: ::   .:: 

C. elegans AKT-1      HTLTENRVLQRCKHPFLTELKYSFQEQHYLCFVMQFANGGELFTHVRKCGTFSEPRARFY 296
(PDB: 4AXA) AKT1      HTLNEKRILQAVNFPFLTKLEFSFKDNSNLYMVMEYAPGGEMFSHLRRIGRFSEPHARFY 147
(PDB: 1O6L) AKT1      HTVTESRVLQNTRHPFLTALKYAFQTHDRLCFVMEYANGGELFFHLSRERVFTEERARFY 110
                      **:.*.*:**  ..**** *::*: :  * :**::* ***:* *: :   *:* :**** 

C. elegans AKT-1      GAEIVLALGYLHRCDIVYRDMKLENLLLDKDGHIKIADFGLCKEEISFGDKTSTFCGTPE 356
(PDB: 4AXA) AKT1      AAQIVLTFEYLHSLDLIYRDLKPENLMIDQQGYIKVTDFGFAKRV---KGRTWTLCGTPE 204
(PDB: 1O6L) AKT1      GAEIVSALEYLHSRDVVYRDIKLENLMLDKDGHIKITDFGLCKEGISDGATMKTFCGTPE 170
                      .*:** :: ***  *::***:* ***::*::*:**::***:.*.        *:***** 
```

*Figure 4* **C. elegans AKT-1 shows good sequence similarity between the two PDB AKT structures 4AXA and 1O6L.** *Sequence alignment of AT13148 binding region between C. elegans AKT-1 canonical form, a Homo sapiens-Bos Taurus chimera of AKT (PDB accession: 4AXA) and a Homo sapiens chimera of AKT (PDB accession 1O6L) run in UniProt. "**\***"*

*indicates perfectly conserved residues, ":" indicates strongly conserved and ".": indicates some conservation between the alignments.*

Detailed analysis of the sequence alignment [Figure 4] between *C. elegans* AKT-1 and the PDB structures 4AXA and 1O6L reveals that *C. elegans* AKT-1 bears close resemblance to the human structure 1O6L, in which ANP is bound [Figure 3]. The majority of differences in sequence in the AT13148 binding region, as identified with the star homology system, appear to originate from differences to the bull-human chimera structure 4AXA in which AT13148 is bound. This highlights both that the AT13148 binding site in *C. elegans* retains high similarity in sequence to the human model, but also that the mechanism in which AT13148 is bound in the structure 4AXA, may not properly represent the true binding mechanism in humans and *C. elegans* forms of AKT.

With this information, we proceeded to test this in vivo [Section 3.2.3].

## 3.1.2. The AKT inhibitor MK2206 has potential to interact with *C. elegans* AKT-1

MK-2206 in contrast to AT13148, binds allosterically to the PH (pleckstrin-homology) domain of AKT [27], inhibiting phosphorylation activity. A sequence alignment [Figure 5] between human and *C. elegans* AKT shows high sequence similarity in the PH domain. No crystal structure is available detailing the binding interactions of MK2206. However M.Rehan et al 2014 [50]use bioinformatics analysis to predict the precise binding sequence. They identify a number of residues involved in the docking of the molecule into the binding site and the final phase binding and these are highlighted in [Figure 5].

```
CLUSTAL O(1.2.4) multiple sequence alignment

Human AKT1        ----------MSDVAIVKEGWLHKRGEYIKTWRPRYFLLKNDGTFIGYKERPQDVDQREA    50
C. elegans AKT-1  MSMTSLSTKSRRQEDVVIEGWLHKKGEHIRNWRPRYFMIFNDGALLGFRAKPKEGQPFPE    60
Human AKT2        ----------MNEVSVIKEGWLHKRGEYIKTWRPRYFLLKSDGSFIGYKERPEAPDQTLP    50
C.elegans AKT-2   ---MSTENAHLQKEDIVIESWLHKKGEHIRNWRPRYFILFRDGTLLGFRSKPKEDQPLPE    57
                       .  :: *.****:**:*:.******::  **::*:: :*:  :

Human AKT1        PLNNFSVAQCQLMKTERPRPNTFIIRCLQWTTVIERTFHVETPEEREEWTTAIQTVADGL   110
C. elegans AKT-1  PLNDFMIKDAATMLFEKPRPNMFMVRCLQWTTVIERTFYAESAEVRQRWIHAIESISKKY   120
Human AKT2        PLNNFSVAECQLMKTERPRPNTFVIRCLQWTTVIERTFHVDSPDEREEWMRAIQMVANSL   110
C.elegans AKT-2   PLNNFMIRDAATVCLDKPRPNMFIVRCLQWTTVIERTFYADSADFRQMWIEAIQAVSSHN   117
                  ***:*  :  :.     :  ::**** *::**************:.::  : *:  *  **: ::.

Human AKT1        KKQ----EEEEMD--------------------FRSGSPSDNSG-----------AEEME   135
C. elegans AKT-1  KGTNANPQEELM--ETNQQPKIDEDSEFAGAAHAIMGQPSSGHGDNCSIDFRASMISIAD   178
Human AKT2        KQR--APGEDPMD--------------------YKCGSPSDSST-----------TEEME   137
C.elegans AKT-2   RLKENAGNTSMQEEDTNGNPS--------GESDVNMD----ATSTRSDNDFESTVMNIDE   165
                  :          .                  .                :

Human AKT1        VSLAKPKHRVTMNEFEYLKLLGKGTFGKVILVKEKATGRYYAMKILKKEVIVAKDEVAHT   195
C. elegans AKT-1  TSEAAKRDKITMEDFDFLKVLGKGTFGKVILCKEKRTQKLYAIKILKKDVIIAREEVAHT   238
Human AKT2        VAVSKARAKVTMNDFDYLKLLGKGTFGKVILVREKATGRYYAMKILRKEVIIAKDEVAHT   197
C.elegans AKT-2   PEEVPRKNTVTMDDFDFLKVLGQGTFGKVILCREKSSDKLYAIKIIRKEMVVDRSEVAHT   225
                      :  :**::*::**::**:.******** :** : **:**::*:::: :.*****

Human AKT1        LTENRVLQNSRHPFLTALKYSFQTHDRLCFVMEYANGGELFFHLSRERVFSEDRARFYGA   255
C. elegans AKT-1  LTENRVLQRCKHPFLTELKYSFQEQHYLCFVMQFANGGELFTHVRKCGTFSEPRARFYGA   298
Human AKT2        VTESRVLQNTRHPFLTALKYAFQTHDRLCFVMEYANGGELFFHLSRERVFTEERARFYGA   257
C.elegans AKT-2   LTENRVLYACVHPFLTLLKYSFQAQYHICFVMEFANGGELFTHLQRCKTFSEARTRFYGS   285
                  :**.***     ***** ***:** :  :****:*.******* *:  : .*:* *:****:

Human AKT1        EIVSALDYLHSEKNVVYRDLKLENLMLDKDGHIKITDFGLCKEGIKDGATMKTFCGTPEY   315
C. elegans AKT-1  EIVLALGYLHRC-DIVYRDMKLENLLLDKDGHIKIADFGLCKEEISFGDKTSTFCGTPEY   357
Human AKT2        EIVSALEYLHSR-DVVYRDIKLENLMLDKDGHIKITDFGLCKEGISDGATMKTFCGTPEY   316
C.elegans AKT-2   EIILALGYLHHR-NIVYRDMKLENLLLDRDGHIKITDFGLCKEEIKYGDKTSTFCGTPEY   344
                  **: ** ***   :*:****:*****:**:******:******* *  *  :.********

Human AKT1        LAPEVLEDNDYGRAVDWWGLGVVMYEMMCGRLPFYNQDHEKLFELILMEEIRFPRTLGPE   375
C. elegans AKT-1  LAPEVLDDHDYGRCVDWWGVGVVMYEMMCGRLPFYSKDHNKLFELIMAGDLRFPSKLSQE   417
Human AKT2        LAPEVLEDNDYGRAVDWWGLGVVMYEMMCGRLPFYNQDHERLFELILMEEIRFPRTLSPE   376
C.elegans AKT-2   LAPEVIEDIDYDRSVDWWGVGVVMYEMMCGRLPFSAKENGKLFELITTCDLKFPNRLSPE   404
                  *****::* **.*.*****:************** ::: :*****   ::;** *. *

Human AKT1        AKSLLSGLLKKDPKQRLGGGSEDAKEIMQHRFFAGIVWQHVYEKKLSPPFKPQVTSETDT   435
C. elegans AKT-1  ARTLLTGLLVKDPTQRLGGGPEDALEICRADFFRTVDWEATYRKEIEPPYKPNVQSETDT   477
Human AKT2        AKSLLAGLLKKDPKQRLGGGPSDAKEVMEHRFFLSINWQDVVQKKLLPPFKPQVTSEVDT   436
C.elegans AKT-2   AVTLLSGLLERVPAKRLGAGPDDAREVSRAEFFKDVDWEATLRKEVEPPFKPNVMSETDT   464
                  * :**:*** : *  :***.* .** *: .   **    : *: .   .*:: **:**:* **.**

Human AKT1        RYFDEEFTAQMITITPPDQDDSMECVDSER--RPHFPQFSYSASGTA-------------   480
C. elegans AKT-1  SYFDNEFTSQPVQLTPPSRSGALATVDEQEEMQSNFTQFSFHNVMGSINRIHEASEDNED   537
Human AKT2        RYFDDEFTAQSITITPPDRYDSLGLLELDQ--RTHFPQFSYSASIRE-------------   481
C.elegans AKT-2   SFFDREFTSMPVQLTPPRRGEELPTVDEEEELQANFIQFASYYVSGSLERSYDTNRSADK   524
                  :** ***:  : :*** :   :    : :: :.  : :* **:

Human AKT1        ----  480
C. elegans AKT-1  YDMG  541
Human AKT2        ----  481
C.elegans AKT-2   YEIR  528
```

Blue: Uniprot identified nucleotide binding site

Yellow:Regions surrounding predicted MK2206 binding cavity

Pink: Residues predicted to be involved in final phase binding of MK2206

Green: Phosphorylated for activation of AKT

Purple: Predicted to be involved in docking of MK2206 into binding site

—— PH domain

*Figure 5 **Most residues involved in MK2206 binding are conserved between human and C. elegans**. Sequence alignment between human and C. elegans AKT1 & AKT2. Blue highlights the region involved in nucleotide binding. Yellow highlights residues immediately surrounding the predicted MK2206 binding cavity. Pink highlights residues predicted to be involved in final phase binding of MK2206. Purple highlights residues predicted to dock MK2206 into the binding site. Green highlights residues that are phosphorylated for activation of AKT1. AKT1 and AKT2 are predicted to have some differences in binding mechanism. "*" indicates perfectly conserved residues, ":" indicates strongly conserved and "." indicates some conservation between the alignments.*

While overall PH domain similarity between Human and *C. elegans* AKT-1 and AKT-2 remains high, my alignment showed that several of the residues and surrounding regions predicted to be required for docking of MK2206 are not conserved in the *C.*

*elegans* proteins. However, as it is possible that elements of protein structure could still be conserved at a level sufficient to allow MK2206 binding, we wanted to explore beyond the primary sequence. As no *C. elegans* AKT-1 or AKT-2 structure was available, Phyre2 was used to generate a prediction of worm AKT-1 which was then overlain with the Human protein in Pymol, with MK2206 positioned in the predicted binding orientation [Figure 6]. This analysis showed that there is a steric clash between Val-244 of worm AKT-1 and the centre of the MK2206 molecule, whereas the equivalent Val-201 of the human protein resides in close proximity to the primary amine. From the sequence alignment [Figure 5], it was apparent that human Lys-268 had no functionally equivalent residue in *C. elegans*; and from the structural prediction by Phyre2, there is also no proximal replacement [Figure 6]. While some of the regions are not well conserved in *C. elegans* AKT-1, much of the sequence and structure are equivalent. In addition, bioinformatics analysis remains subservient to crystallography and NMR techniques, predicting the nature in which MK2206 with interact with the *C. elegans* form of AKT-1 remains uncertain. Thus, despite the possibility raised by the in-silico analysis that MK2206 may not interact with the worm version of AKT-1 we decided to persevere and test it for any *in vivo* effects in parallel with AT13148 [Section 3.2.4].
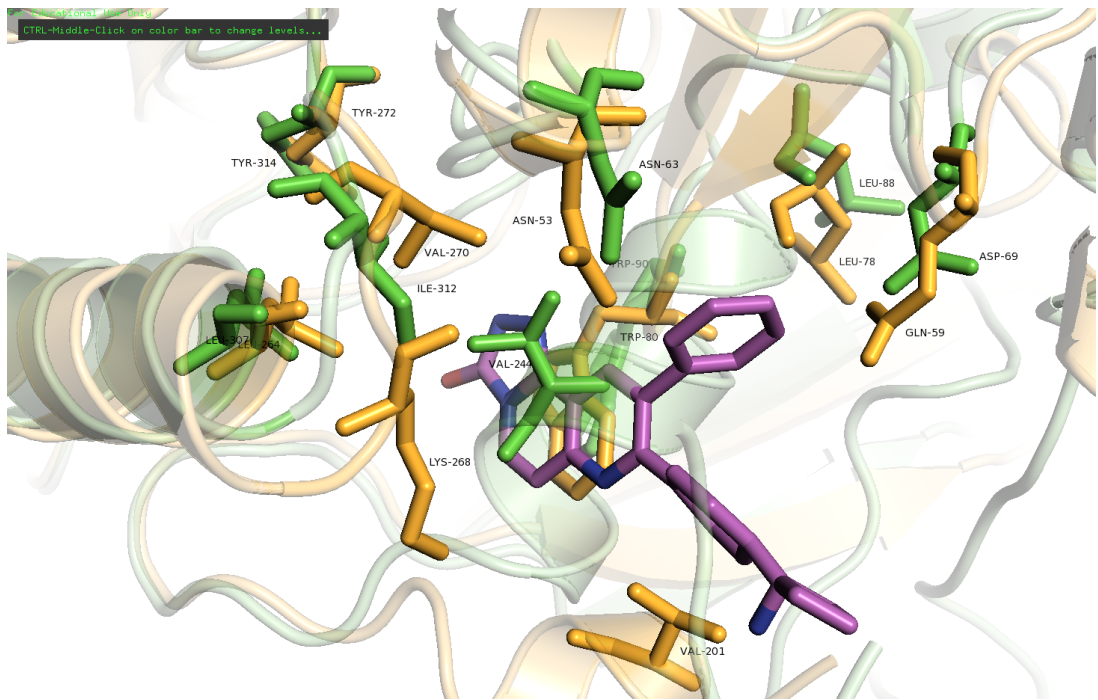
*Figure 6 **The predicted structure for C. elegans AKT-1 shows several differences in structure to human AKT1 at the MK2206 binding pocket.** Overlay between all backbone atoms of human AKT1 crystal structure (3o96) and PHYRE2 predicted C. elegans AKT-1 structure with the predicted MK2206 binding array (observed in Pymol). MK2206 in purple, human AKT1 binding residues in orange and C. elegans equivalent residues in green*

## 3.2. AKT inhibitors AT13148 and MK2206 affect *E. coli* growth but do not induce nuclear localisation of DAF-16

The ability of the drugs to target the insulin signalling pathway was tested in worms. This was determined by scoring the extent of nuclear localisation of *DAF-16::GFP*; under a fluorescent microscope on the scale of low, medium and high localisation to the nucleus [Figure 7].
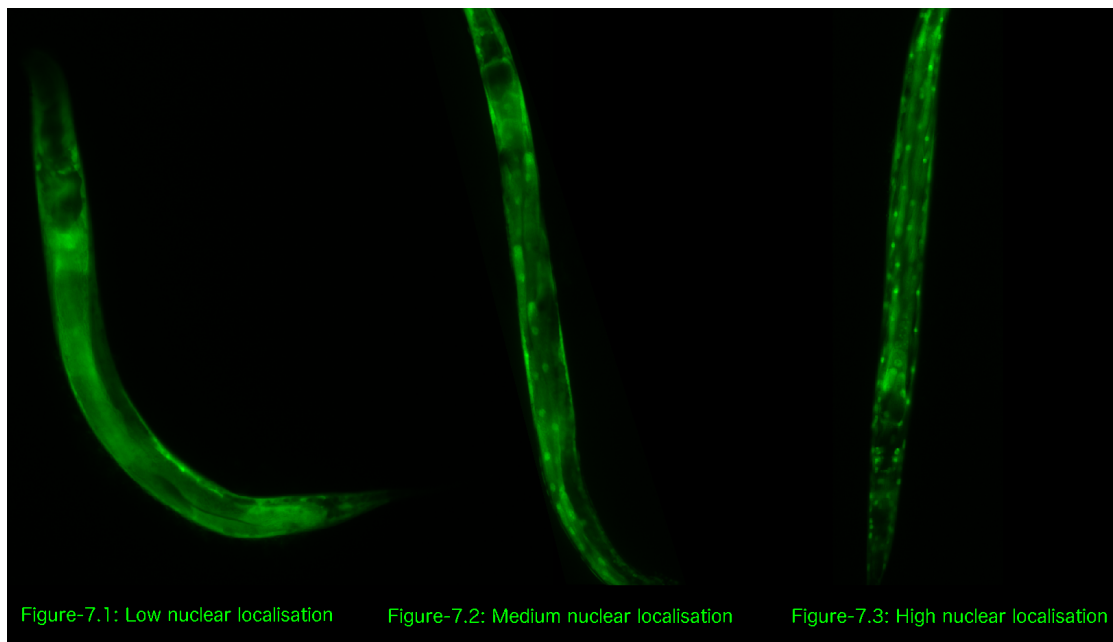
*Figure 7* **Example of scoring of DAF-16 nuclear localisation.** *Figure-7.1, representing low nuclear localisation, shows no DAF-16::GFP dispersed throughout the cytoplasm. Figure-7.2, representing medium nuclear localisation, shows a mixture of cytoplasmic and nuclear DAF-16::GFP. Figure-7.3, representing high nuclear localisation: the majority or all of DAF-16::GFP is localised to the nucleus.*

## 3.2.1. 2.5% DMSO is an acceptable solvent concentration for worms

DMSO is a harsh chemical used as a solvent for drug delivery and has been established to be toxic at concentrations as little as 0.1% in some circumstances[51]; an insufficient concentration to solubilise an amount of drug affective against *C. elegans*. Because of this and because DAF-16 functions primarily in response to stress, it must be confirmed that DMSO does not induce DAF-16 nuclear localisation through stress instead of as a result of AKT inhibition from the drug and is not observed to cause effects relating to toxicity. Both the drugs AT13148 and MK2206 are solubilised in DMSO, finding the tolerance of worms to DMSO was necessary to determine the maximum concentration that could be safely used without influencing DAF-16 nuclear localisation. This was carried out by subjecting worms to several concentrations of DMSO, at and past the maximum concentration used in the assays and screening for any localisation. The proportion of dead worms was also counted to test for the extent of toxicity of DMSO on the worms. If levels of nuclear localisation and the number of deaths

deviate insignificantly from the control group at DMSO concentrations used in the assay, then DMSO will be deemed to be viable as a solvent.

It must also be confirmed that the drugs do not induce nuclear localisation and longevity as a stress response instead of specific inhibition of AKT.
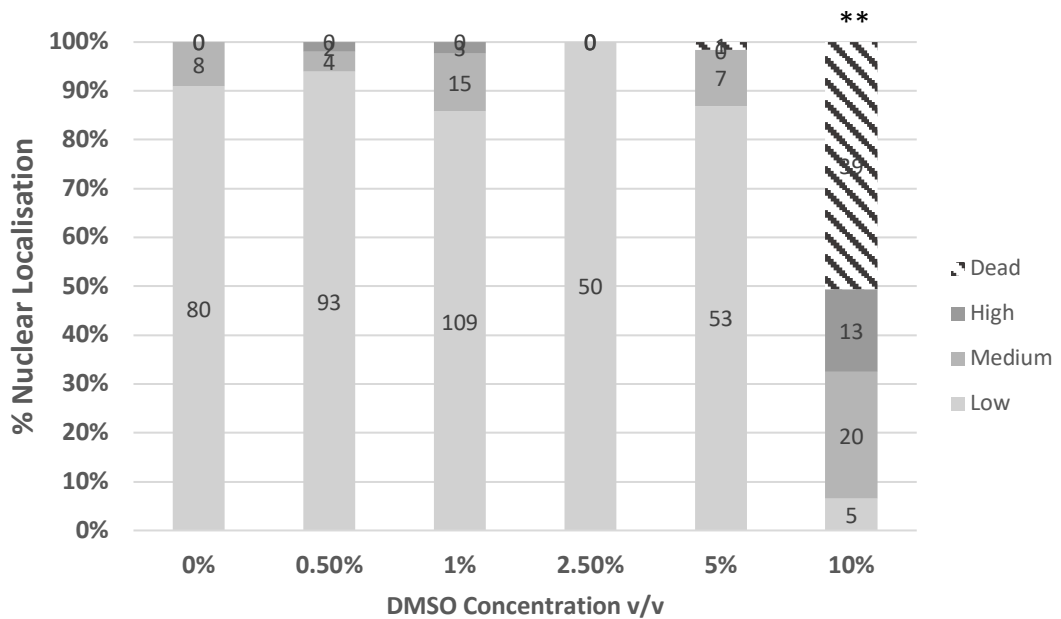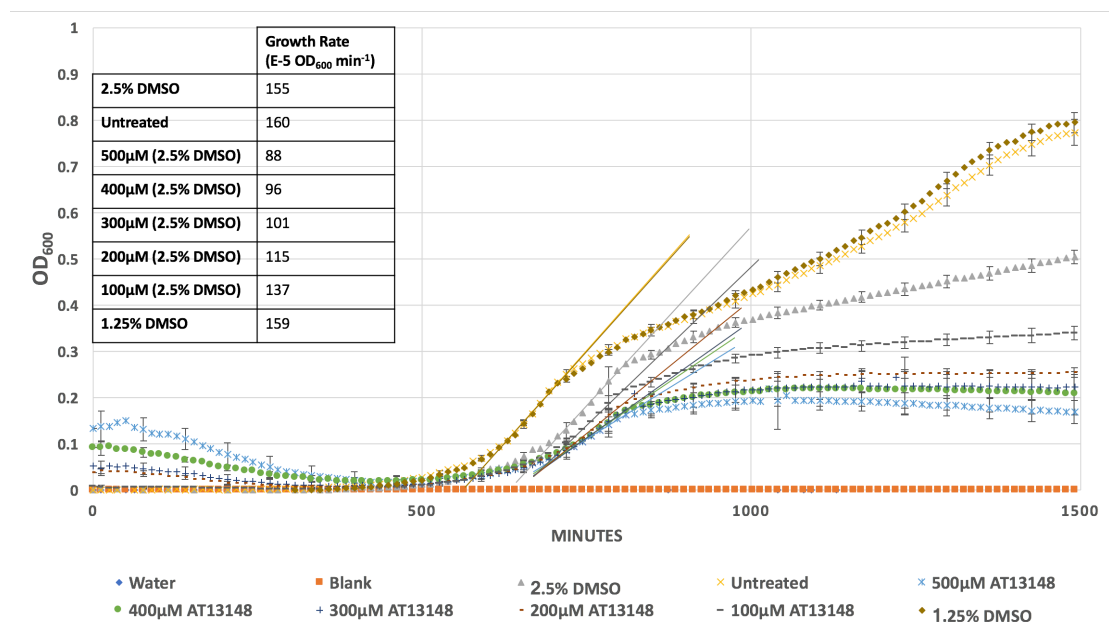


*Figure 8 **Up to 5% DMSO does not influence DAF-16 localisation to the Nucleus.** Effect on nuclear localisation of DAF-16 from 24hr incubation of C. elegans JMT10 strain (bus-8) with concentrations of DMSO ranging from 0 to 10 percent (v/v). Low, medium and high refer to the magnitude of nuclear localisation of DAF-16 and dead refers to worms with deaths attributed to the incubation. * represents ≥95% confidence that any variation in data from the control (0%) was not due to chance and so the null hypothesis, that the two sets of data are the same, is rejected (Kruskal-Wallis and one-tail Dunnetts post-hoc); ** represents ≥ 99% confidence. Worm count is indicated in each bar.*

Figure 8 shows the results of incubation of worms with different concentrations of DMSO in liquid media over 24 hours. Up to 5% DMSO in liquid media showed no change in DAF-16 nuclear localisation. At 10% most worms were reported as dead at the end of incubation, showing no movement or response to touch; the living worms showed medium and high degrees of localisation. The data shows that 5% DMSO was the maximum percentage that did not affect the background levels of DAF-16::GFP nuclear localisation. A concentration of 2.5% DMSO is therefore unlikely influence the nuclear localisation of DAF-16::GFP when used as a solvent

for the drugs and will allow administration of a substantial maximum drug concentration of 500µM from the stock solution of 20mM.

## 3.2.2. AT13148 and MK2206 both influence *E. coli* growth

As worms were fed with live *E. coli* It was also necessary to determine the effect the drugs posed on the growth of the bacteria. Exposing the bacteria to the drugs has the potential to result in altered bacterial gene expression and metabolism in an effort to mitigate the effects of the compound, which ultimately may affect both the nutrient content of the bacteria and the concentration and or result in biotransformation of the drug, which would nullify the test conditions[52] [53]. To test the effect of the AKT inhibitor drugs on bacterial growth, OP50 bacteria were grown in different concentrations of drug in liquid S-medium and optical density at 600nm was measured at ~13 minute intervals for a total time of 25 hours. The growth rate in each condition was determined from the slope of log phase, the values for which located in the table in each of figures 9&10.



| | Growth Rate (E-5 $OD_{600}$ $min^{-1}$) |
|---|---|
| 2.5% DMSO | 155 |
| Untreated | 160 |
| 500µM (2.5% DMSO) | 88 |
| 400µM (2.5% DMSO) | 96 |
| 300µM (2.5% DMSO) | 101 |
| 200µM (2.5% DMSO) | 115 |
| 100µM (2.5% DMSO) | 137 |
| 1.25% DMSO | 159 |

*Figure 9* **AT13148 reduces growths rate of log phase. E. coli, OP50 strain, growth in the presence of various concentrations of AT13148**. *Growth rate was obtained from the slope of log phase; values for growth rate are displayed in the table as a change in optical density over time. Data from three combined technical replicates of one biological replicate. Error bars show standard deviation between technical repeats. Representative trial, repeats in appendix.*

The maximum DMSO concentration of 2.5% appeared to show little effect on the bacteria's growth rate, compared to the untreated control but did show a slight extension of lag phase [Figure 9]. However, both other repeats indicated a higher growth rate of the untreated to that of the DMSO treated, with values comparable to the untreated in the MK2206 data [Figure 10]. DMSO therefore appears to both extend lag phase and slow log phase.

As the concentration of AT13148 increased, a roughly linear, inverse effect on growth rate was observed, with bacteria treated with 500µM of drug having a growth rate of around 65% of bacteria treated with 100µM. Maximum growth density appeared severely reduced in the DMSO control growth and further reduced in the drug groups; the 500µM treated reaching growth density of less than a quarter of the untreated after 1500 minutes (25 hours). Interestingly AT13148 appeared to have no effect on lag phase with log phase initiating simultaneously among all drug trials and the solvent control. While AT13148 was observed to affect bacterial growth, it appeared to deviate little from the 2.5% DMSO control, other than a reduction in maximum growth density. It is therefore unlikely to influence how the drug affects the worms, so long as sufficient quantities of the bacterial food are provided.
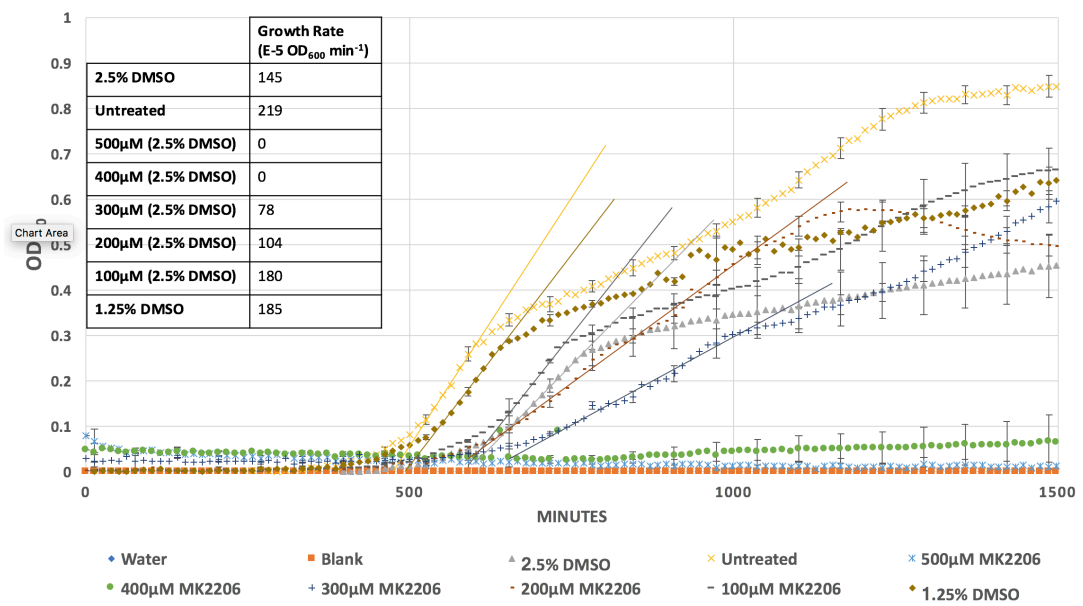


| | Growth Rate (E-5 OD$_{600}$ min$^{-1}$) |
|---|---|
| 2.5% DMSO | 145 |
| Untreated | 219 |
| 500µM (2.5% DMSO) | 0 |
| 400µM (2.5% DMSO) | 0 |
| 300µM (2.5% DMSO) | 78 |
| 200µM (2.5% DMSO) | 104 |
| 100µM (2.5% DMSO) | 180 |
| 1.25% DMSO | 185 |

*Figure 10 MK2206, up to 300µM, causes erratic growth of E. coli and inhibits growth at 400µM. E. coli, OP50 strain, growth in the presence of various concentrations of MK2206. Growth rate was obtained from the slope of log phase; values for growth rate are displayed*

*in the table as a change in optical density over time. Data from three combined technical replicates of one biological replicate. Error bars show standard deviation between technical repeats. Representative trial, repeats in appendix.*

The presence of MK2206 greatly affected growth of *E. coli*, more so than AT13148; above 400μM causing complete inhibition of growth [Figure 10]. The pattern of growth amongst the different concentrations was considerably more erratic than observed with AT13148. The 2.5% DMSO control group showed much a similar curve and growth values as seen before. 100μM MK2206 appeared to then show an increased growth rate and greater maximum OD. Whilst growth rate at 200μM and 300μM was decreased when compared to the DMSO solvent control, log phase wass considerably extended, resulting in the density of bacteria at these two concentrations to surpass. It was concluded that concentrations at 300μM or above of MK2206 affected bacterial growth too greatly for any meaningful data to be generated from testing these concentrations of worms. While 100μM and 200μM also affected growth, the extent to which was much less. It was considered that if the effect observed on the worms, at these concentrations, was great enough, the extent likely caused by the bacteria would be minimal.

### 3.2.3. AT13148 does not induce nuclear localisation of DAF-16

Increased lifespan in worms, through reduced insulin/insulin-like signalling (rIIS), has been shown to require DAF-16 activity. However, genetic modification of this signalling pathway would not be an ideal approach to duplicate this effect in humans. We looked at whether the AKT inhibitors AT13148 and MK2206 could be used to imitate rIIS, pharmaceutically in worms. We initially tested whether these drugs induce nuclear accumulation of DAF-16 through inhibition of AKT, by using a DAF-16::GFP overexpressing strain of worms and observing the extent of nuclear localisation using fluorescent microscopy.

One issue is that wild type *C. elegans* are highly resistant to diffusion of small molecules across their cuticle and so require high drug concentrations for physiological effects to be seen. Previous research has identified *bus-8* mutants to have a defective cuticle, facilitating small molecule diffusion and permitting lower

concentrations of drugs to be administered for a physiological effect to be observed.
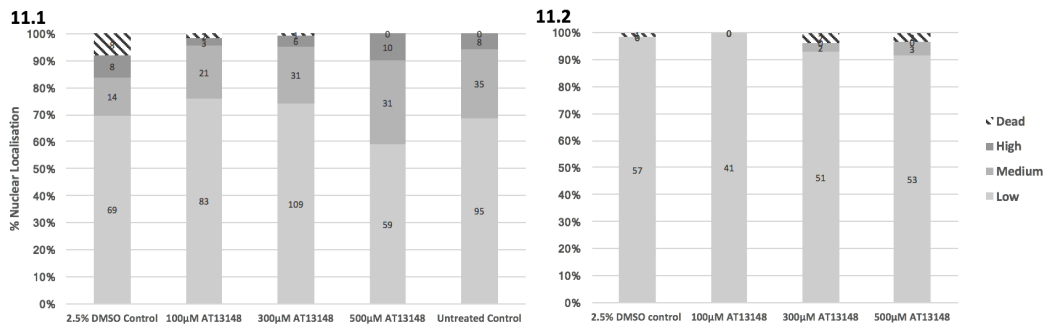


*Figure 11 **The presence of AT13148 does not influence nuclear localisation of DAF-16.** Degree of nuclear localisation of DAF-16::GFP of JMT10 (bus-8) strain after incubation with AT13148. **11.1** shows the combined data of the initial four repeats, **11.2** shows a later fifth repeat after changes to the protocol were made to constrain background levels of DAF-16 nuclear localisation. Worm count is indicated in each bar. \*\* = p <0.01*

When trialling AT13148 with *bus-8* worms, no difference in the nuclear localisation of DAF-16 from the control was observed after incubation with up to 500µM of drug (Figure 11.1). The initial data set however suffered from inconsistencies (not shown) and frequently, unusually high background nuclear localisation in the control group. This effect was not initially seen when testing AT13148 nor observed in the DMSO tolerance assay. After alterations to the protocol, replacing distilled water in the agarose pads and in the tetramisole hydrochloride with M9 buffer and replacing stock reagents, the experiment was repeated a fifth time (Figure 11.2). Background levels of nuclear localisation appear to have decreased dramatically which is now suspected to have been attributed to osmotic stress. And comparably high DAF-16 nuclear localisation and deaths in the control have disappeared. However, the extent of nuclear localisation among any of the drug concentrations trialled still did not differ from the solvent control group (Figure 11.2), which suggests that AT13148 does not activate DAF-16 in worms.

## 3.2.4. MK2206 does not induce nuclear localisation of DAF-16

Testing MK2206 was conducted in the same manner to the revised protocol created when testing AT13148.

As 300μM of MK2206 or above was observed to severely impair *E. coli* growth
[Figure 10], 100μM and 200μM were the only concentrations of MK2206 trialled on
worms; testing only 100μM and 200μM MK2206 on worms meant the
concentration of DMSO within the liquid media could be reduced down to 1% v/v
from the 20mM stock of MK2206. Although 2.5% DMSO was identified not to
influence DAF-16 activity, minimising the solvent concentration remained
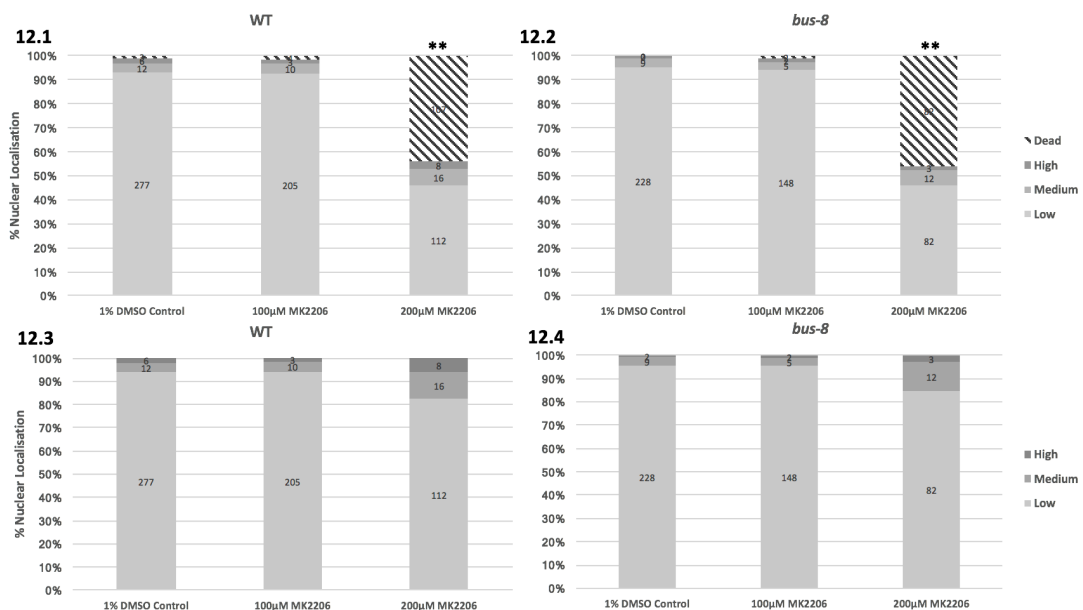advantageous in reducing any potential stresses on the worms.



*Figure 12 Degree of nuclear localisation of DAF-16::GFP after incubation with MK2206. The
trial was conducted thrice with bus-8 mutant (JMT10) and thrice with WT variants (TJ356)
of a daf-16::GFP overexpressing strain. The combined results are displayed in **12.1** and **12.2**
respectively. **12.3**&**12.4** represent **12.1**&**12.2** respectively if dead worms were to be
discounted. ** = p <0.01.*

As with AT13148, Kruskal-Wallis analysis indicated there was not enough evidence
to support the hypothesis that MK2206 induced the nuclear localisation of DAF-16
at 100μM in *bus-8* worms [Figure 12.2].  At 200μM, MK2206 showed high toxicity,
with almost 50% of worms being classed as dead after incubation [Figure 12.2]. If
the dead worms were to be discounted from the experiment [Figure 12.4], the
extent of DAF-16::GFP nuclear localisation is still insufficient to state a difference.
Unlike with AT13148, 200μM MK2206 caused a high proportion of the *bus-8*
(JMT10) worms to die during incubation [Figure 12.2]. MK2206 was trialled on the
WT (TJ356) [Figure 12.1&12.3] worms to test if the more integral cuticle of this

strain may benefit survival. No difference in the extent of nuclear accumulation or proportion of deaths was seen between the WT and *bus-8 mutants*.

In conclusion, MK2206 does not induce DAF-16::GFP entry into the nucleus.

## 3.3. SKN-1B characterisation

### 3.3.1. *skn-1b* contributes to foraging behaviour

SKN-1 is the functional orthologue to the Nrf2 transcription factor and functions as an effector downstream of insulin signalling, alongside DAF-16. *skn-1* has 4 isoforms, of which only *skn-1b* is required for DR induced longevity [42]. In addition, current (unpublished) research identifies *skn-1b* to be required for rIIS lifespan extension. Despite this, little is known about skn-1b's precise activity. As *skn-1b* is important for dietary restriction (DR) and is expressed in the ASI chemosensory neurons, it is possible that it is involved in how *C. elegans* responds to food, either sensory or behavioural, which may ultimately influence DR. To test the hypothesis that *skn-1b* is involved in feeding behaviour, an assay was set up to determine how *skn-1b* and N2 (WT) worms food seeking behaviour changes as they age. To carry this out, the ratio of worms foraging, to situated on the bacterial lawn, was recorded each day. This experiment was repeated with both an OP50 and HT115, *E. coli* food source.
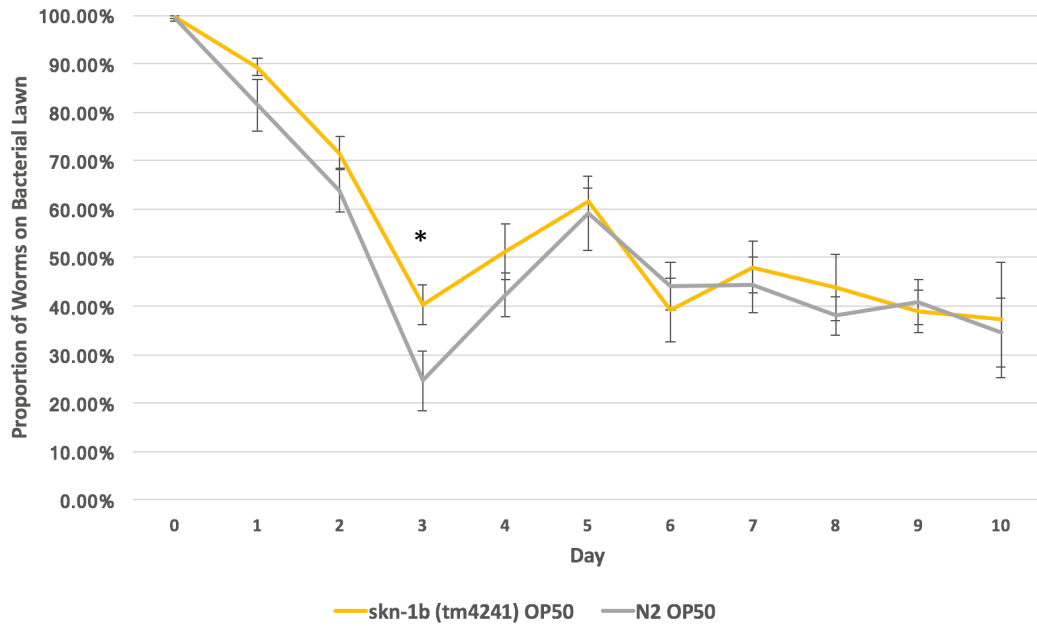
*Figure 13* **N2 (WT) worms show more foraging behaviour than skn-1b worms in early life on OP50 bacteria.** *Y-axis shows the proportion of worms on the bacterial lawn on observation. The X-axis indicates the day of observation. Day zero represents the L4 worms counted 1 hour after plating. Error bars show standard error of the mean. Pooled data from three repeats up to day 4 and two repeats thereafter. Initial worm count >220 worms total in each condition. * = p <0.05.*
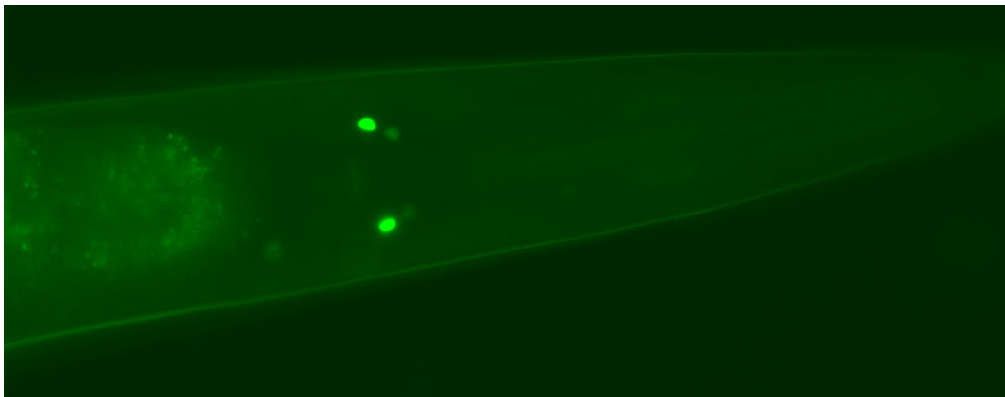
Over the first 6 days of the experiment, a higher proportion of skn-1b mutant worms remained on the OP50 lawn than N2. As they aged this difference subsided and both N2 and SKN-1B worms displayed similar foraging behaviour [Figure 13]. However, the different was only found to be significant by T-Test at day 3 of adulthood.
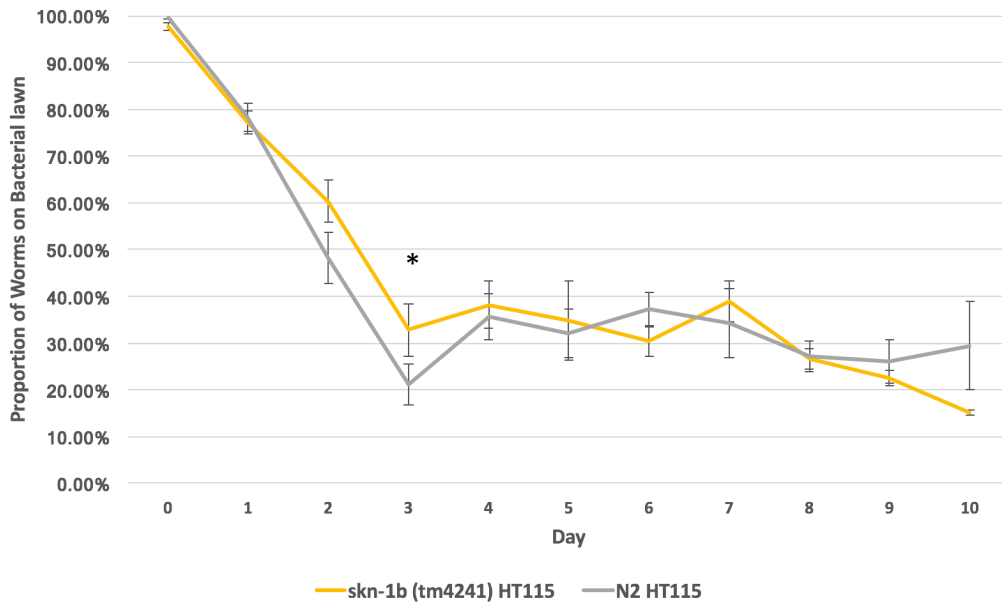
*Figure 14* **N2 (WT) worms show more foraging behaviour than skn-1b worms in early life on HT115 bacteria.** *Y-axis shows the proportion of worms on the bacterial lawn on observation. The X-axis indicates the day of observation. Day zero represents the L4 worms counted 1 hour after plating. Error bars show standard error of the mean. Pooled data from three repeats up to day 4 and two repeats thereafter. Initial worm count >220 worms total in each condition. * = p <0.05.*

This experiment was repeated using HT115 strain of *E. coli,* usually used for conducting RNA interference (RNAi). Different bacteria are constituted of different nutritional values and worms respond differently both behaviourally, favouringly one strain over another[54],[55] and physiologically, influencing health and longevity[56],[57]. We were curious as to whether *skn-1b* deficient worms respond differently, in comparison to the N2 (WT), to a different bacterial food source.

On HT115 *E. coli [Figure 14]*, SKN-1B and N2 worms show a similar pattern of foraging behaviour to on OP50 [Figure 13] with SKN-1B worms tending to remain more on the lawn in early life than N2. Again, this difference subsided as the worms aged and was only identified as significant at day 3.

There was also observed to be a higher proportion of worms remaining on OP50 bacteria than HT115 over the course of the experiment, which may reflect a general preference for for OP50 over HT115.
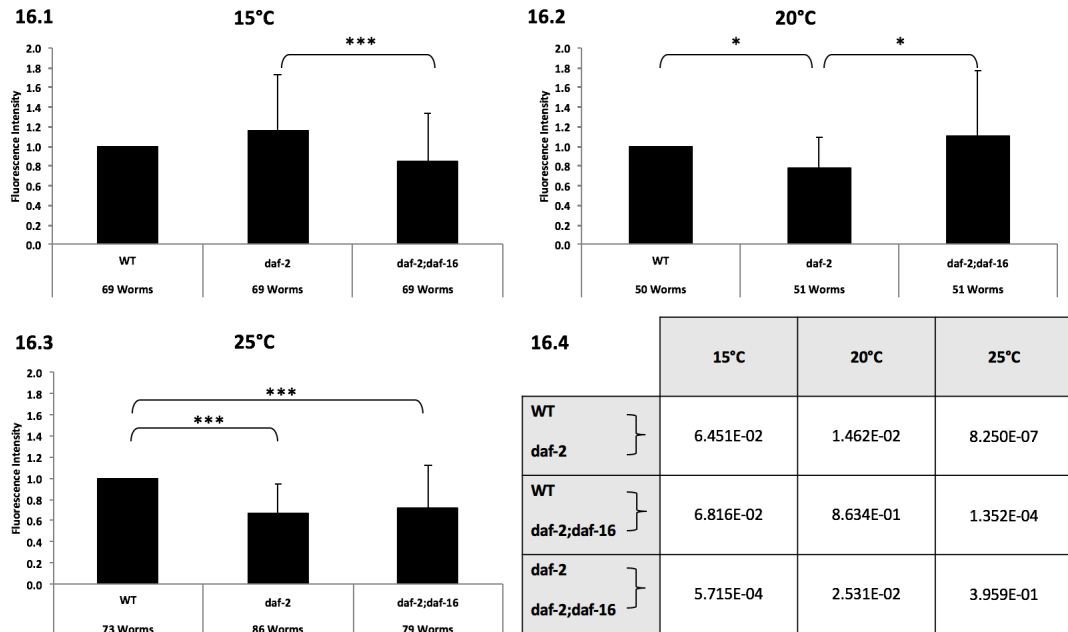
The data leads to the suggestion that *skn-1b* deficient worms exhibit increased dwelling behaviour, tending towards remaining on the lawn more than the wild type.

## 3.3.2. SKN-1B::GFP expression levels are altered in response to insulin signalling, dependent on temperature

Along with DAF-16, some SKN-1 isoforms have been identified to act as a transducer for IIS [Figure 1]. To see whether SKN-1B expression levels were altered in response to reduced IIS I analysed the expression of a SKN-1B::GFP transgene in WT, *daf-2* mutant and *daf-2;daf-16* double mutant worms. As SKN-1B is tagged with GFP, the expression pattern of SKN-1B can be monitored. SKN-1B::GFP is expressed predominantly in the ASI neurons [Figure 15]. Then the level of neuronal accumulation of GFP can be quantified in the different genetic backgrounds using quantitative fluorescence microscopy. Many *daf-2* mutations are temperature sensitive and exhibits different "strengths" at different temperatures[58]. The mutant we use, *daf-2(e1370)*, is not considered temperature sensitive and so the extent of lifespan extension remains constant regardless of temperature, as well as exhibiting no low temperature induced dauer entry. However current unpublished data indicates *daf-2(e1370);skn-1b(tm4241)* mutant worms may be temperature sensitive, so the experiment was carried out at different incubation temperatures [Figure 16].



*Figure 15 **Expression of SKN-1B::GFP in the ASI neurons.***

**16.1** — 15°C

Fluorescence Intensity

| WT 69 Worms | daf-2 69 Worms | daf-2;daf-16 69 Worms |

*** (daf-2 vs daf-2;daf-16)

**16.2** — 20°C

Fluorescence Intensity

| WT 50 Worms | daf-2 51 Worms | daf-2;daf-16 51 Worms |

* (WT vs daf-2)   * (daf-2 vs daf-2;daf-16)

**16.3** — 25°C

Fluorescence Intensity

| WT 73 Worms | daf-2 86 Worms | daf-2;daf-16 79 Worms |

*** (WT vs daf-2)   *** (WT vs daf-2;daf-16)

**16.4**

|  | 15°C | 20°C | 25°C |
|---|---|---|---|
| WT / daf-2 | 6.451E-02 | 1.462E-02 | 8.250E-07 |
| WT / daf-2;daf-16 | 6.816E-02 | 8.634E-01 | 1.352E-04 |
| daf-2 / daf-2;daf-16 | 5.715E-04 | 2.531E-02 | 3.959E-01 |

*Figure 16* **SKN-1B::GFP is regulated differently in response to rIIs at different temperatures.** *Mean SKN-1B::GFP fluorescence intensity in WT, daf-2 and daf-2;daf-16 mutant backgrounds after 24 hours incubation at either 15°C (**16.1**), 20°C (**16.2**) or 25°C (**16.3**). Table (**16.4**) contains p-values from T-tests between each strain. Error bars indicate standard deviation. * = p <0.05, *** = p <0.001*

The data showed that at an incubation temperature of 15°C, SKN-1B::GFP fluorescence in the ASI showed no significant difference in *daf-2* and *daf-2;daf-16* backgrounds to the WT.

At an incubation temperature of 20°C SKN-1B levels in the *daf-2* background dropped compared with the WT (p=0.0146) dependent on *daf-16* (p=0.0253). At 25°C a drop was observed in both the *daf-2* (p=<0.0001) and *daf-2;daf-16* (p=0.000135) backgrounds compared to WT. As the strength of the *daf-2* mutation increases with higher temperature, the IIS pathway is reduced more strongly at higher temperature. Thus, the data would suggest that DAF-2 signalling helps maintain SKN-1B levels in the ASIs.
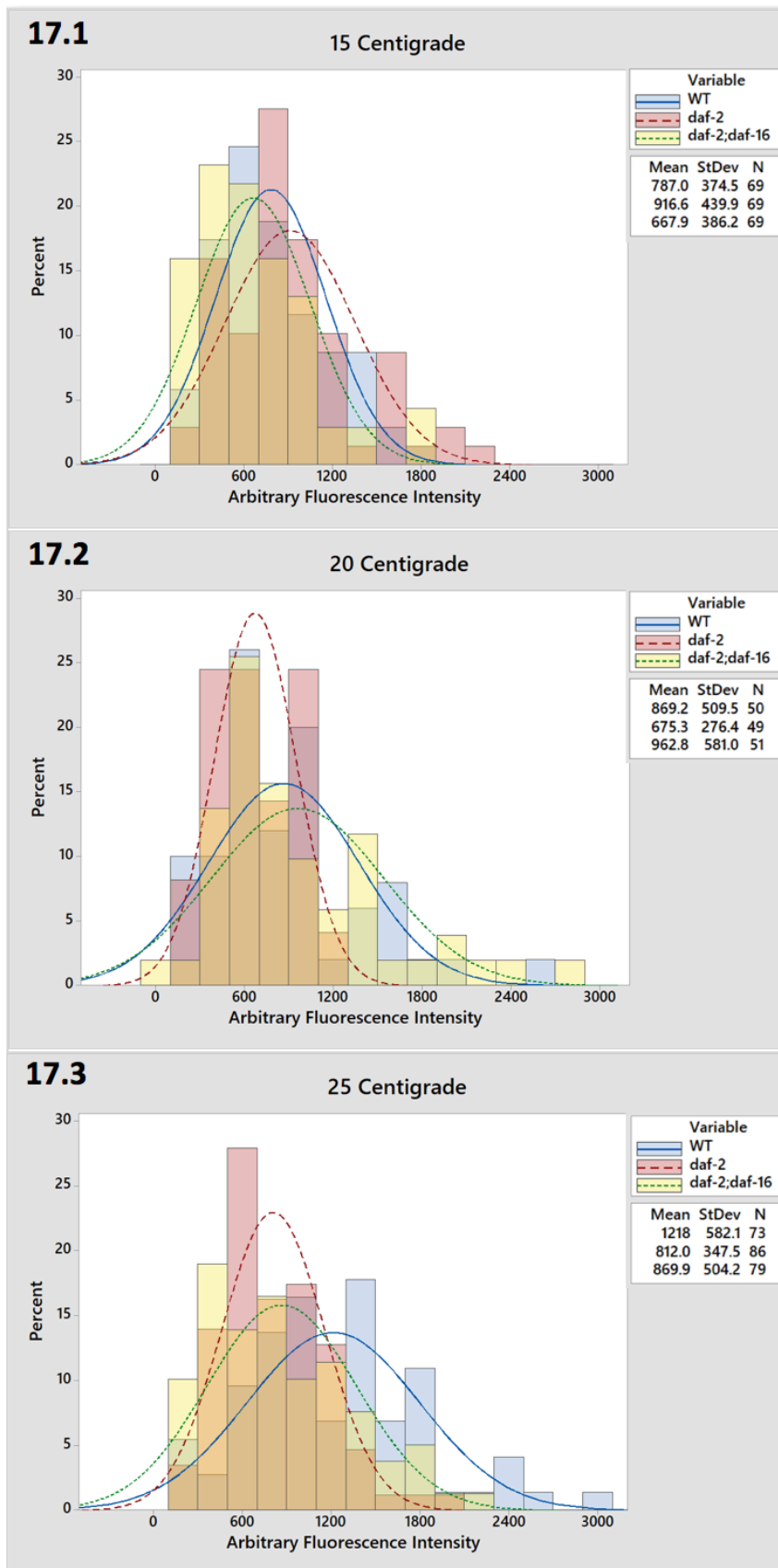
*Figure 17 Distribution of SKN-1B::GFP fluorescence intensity of individual worms in WT, daf-2 and daf-2;daf-16 mutant backgrounds after 24 hours incubation at either 15°C (**17.1**), 20°C (**17.2**) or 25°C (**17.3**).*

Whilst conducting these experiments, it was noted that there was a large amount of variation in SKN-1B::GFP expression between worms. Looking at how the fluorescence was distributed in the different conditions provided a better understanding of the data [Figure 17]. At 15°C all backgrounds showed a similar distribution, *daf-2* appeared slightly more skewed towards higher fluorescence but not significantly different. At 20°C the range of fluorescence of *daf-2* appeared lower than at 15°C with fewer worms showing higher fluorescence. However both the wild type and *daf-2;daf-16* showed a much broader range of fluorescence values and a higher maximum. At 25°C this broadening of the normal distribution became more prominent in the WT but appeared to disappear in the *daf-2;daf-16* background. While *daf-2* retained a similar distribution to at 20°C. The distribution data also highlights how variable the levels of SKN-1B::GFP were, in the same conditions. Out of 3 repeats at 15°C and 25°C and two repeats at 20°C, the data largely failed to remain consistent, with ANOVA reporting significant variation in the repeats of *daf-2* and *daf-2;daf-16* at 15°C and *daf-2* at 25°C. Although variation in neurone fluorescence was high between individual worms, which has likely resulted in variable repeat data, the total number of worms measured in each condition should be sufficient to minimise the impact of this variation and provide a good preliminary data set to how SKN-1B is regulated by rIIS. However, more data should be collected in order to reliably determine the extent of rIIS influence on SKN-1B.

## 4. Discussion

### *C. elegans* as a model for pharmacological activity of MK2206 and AT13148

An effect was exerted by the presence of both AT13148 and MK2206 on the growth of bacteria particularly at 300μM and above of MK2206. However, this effect was thought to be minor for AT13148 and at 200μM MK2206. It was considered that if high effect on DAF-16 activation was observed the influence from bacteria would be negligible. It is unusual though, that no induction of DAF-16::GFP to the nucleus was observed, at least with AT13148. The ATP binding

pocket is very well conserved between species and a crystal structure of AT13148 bound shows that many of the same residues required to interact with ATP are involved in the interaction with AT13148. Inhibition of AKT-1 should result in DAF-16 no longer being sequestered in the cytoplasm and therefore translocate to the nucleus. As DAF-16::GFP was not observed to accumulate in the nucleus to any extent, it would suggest AKT-1 was not being inhibited. Although AKT-1 is not the soul regulator of DAF-16 [17],[59], as other pathways have been shown to have influence, some effect would have expected to have been observed if AKT-1 was inhibited. It is possible that the involvement of bacterial or worm biotransformation was greater than anticipated and that after 24 hours incubation the effects of the drugs had dissipated. It may be possible to use NMR spectroscopy to quantitate drug decay at various time points of the assay which would provide a better representation of how the drug is metabolised than measuring bacterial growth. Although no effect was observed with concentrations up to 500µM AT13148, a large proportion of worms were reported dead after incubation with 200µM MK2206 but with no effect at 100µM. It's unknown whether this was down toxicity of MK2206 or biotransformation products.

It was observed when the bacteria and either of the drugs were mixed in liquid media, that the bacteria would clump strongly, becoming more prominent with increasing concentration. This may explain the unusually high $OD_{600}$ values during the initial lag phase period seen with the bacterial growth curves. It may also give an indication to the toxicity of the drugs towards the bacteria as clumping together would reduce the total surface area exposed to the surrounding drugs and may have been adopted as a survival strategy of the bacteria[60].

## Contribution of *skn-1b* to foraging behaviour

Although it was determined skn-1b expression likely contributes to foraging behaviour, the large variation between samples does weaken confidence in the reliability. To overcome, this would require a larger data set, either by repeating many times or by increasing the observation number for each day. In addition, live bacteria were used as a food source; over time the bacteria is trailed across the plate forming minor lawns over time, causing indefinite and often skewed data.

One experiment (data not shown), in which the worms were transferred to fresh plates at day 5, showed a sharp increase in the number of worms on the bacterial after re-plating, suggesting worms were being encouraged off the lawn by the trailed bacteria. This may also be the cause of the difference observed between the OP50 and HT115, as HT115 grows more vigorously on NGM, so the trails left by the bacteria grow stronger and there is less encouragement for worms to return to the lawn. Using killed bacteria for both the assay and for prior maintenance of the worms may constrain this in future.

A recent paper by Wilson et al 2017 [61] identified that *skn-1(zu67)* mutants show increased sensitivity to small quantities of bacteria and tended to dwell more on the bacteria rather than seek out potential new food sources when bacterial density was limited. This is similar to what we have found with *skn-1(tm4241)*, where an increased proportion of worms remained on the lawn to the wild type (N2), in early life. However, no difference in foraging behaviour was observed 1 hour after transfer of *skn-1(tm4241)* worms to the assay plate as was observed by Wilson et al with *skn-1(zu67)*. This may be down to the difference in set up of the assays in which s*kn-1(zu67)* was plated with highly diluted bacteria, whereas *skn-1(tm4241)* was plated with a full bacterial lawn and so bacterial density was not limited. In addition, the *zu67* mutation relates to loss of function of *skn-1a* and *skn-1c* and not skn-1b, as *tm4241* does. This raises the question of how *skn-1b* worms might respond to limited food. This does also lessen the likelihood that the decrease in lifespan extension of DR worms, as a result of *skn-1b* knockdown, originates from changes in foraging behaviour. If the foraging behaviour was required it would be expected that either rescue of *skn-1a/skn-1c* would recover the lifespan extension or that rescue of solely *skn-1b* would be insufficient for recovery; but that the *skn-1b* isoform appears solely responsible for the lifespan extension seen in DR worms, despite all isoforms being required for WT foraging behaviour to some degree, suggests *skn-1b* is acting in a manner independent of foraging behaviour in this instance. If *skn-1b* is indeed involved in food seeking. It would be interesting to determine what the consequences on physiology would be. As skn-1b is implicated in rIIS longevity, the original intention was to measure behaviour in *daf-2(e1370)* and *daf-2(e1370);skn-1b(tm4241),* in addition to the N2

and *skn-1b(tm4241)*. Problems with the maintenance of these two strains meant they were excluded from the experiment.

## Regulation of SKN-1B by rIIS in response to temperature

rIIS was found to regulate SKN-1B in the ASI neurons at different temperatures. Current, unpublished data suggests that *skn-1b* contributes to lifespan extension, by rIIS, at 15°C but is superfluous to this extension at 20°C. This is interesting, as at 15°C, SKN-1B::GFP abundance in the neurons remained unchanged in the *daf-2* background compared to the WT but at 20°C, abundance was found to be decreased in the *daf-2*. Why SKN-1B should be downregulated at 20°C and 25°C in *daf-2* mutants but not at 15°C and why this effect is only dependant on DAF-16 at 20°C remains unclear.

However, it is also unclear whether this effect would be as a result of altered *skn-1b::GFP* expression or altered turnover rates. Repeating the experiment with a *Pskn-1b::GFP* transcriptional, rather than translational, variant may give an indication. This transgene would express unbound GFP under control of the *skn-1b* promoter in contrast to expression of SKN-1B::GFP. If the changes observed were due to differing *skn-1b* expression across the three backgrounds it would be expected that the differences are retained in the unbound GFP variants. Whereas differing SKN-1B turnover rates should not influence free GFP and as long as *skn-1b* promotion was consistent among the three backgrounds so too should GFP intensity. Alternatively quantitative reverse transcriptase polymerase chain reaction (qRT-PCR) can be used to quantitatively determine expression of *skn-1b* mRNA in each condition. This involves reverse transcription of the mRNA into cDNA before carrying out qPCR. Regarding turnover of SKN-1B as a mechanism of regulation, it has been identified that WDR-23 proteins bind the DIDLID motif of SKN-1 and target it for proteasome degradation[37]. SKN-1B lacks this motif, so it is unclear how this process will operate.

It has been identified that activation of DAF-16 slows overall protein turnover within *C. elegan*[62]*s*. Our data shows that at 20°C SKN-1B::GFP abundance is reduced in the ASI neurons under rIIS but not when DAF-16 is knocked down. However turnover rates and protein abundance are not necessarily correlated as

reduced translation may also accompany reduced turnover rates resulting in no overall protein change.

Despite finding a difference in overall neurone fluorescence, there was a lot of variation in the data. One potential cause may lie with the orientation of the worm. When mounted on the slide for imaging, there is no procedure in place to position the worms uniformly and so variations in the distance and amount of tissue between the neurones may vary. IdC. Cáceres et al 2012 identified a way to laterally orientate worms for imaging[63]. Altering the apparatus may provide a means to more consistently orientate the worms vertically in the optimum position for viewing the ASI neurones.

The *Pskn-1b*::*skn-1b*::GFP transgene is non chromosomal and so copy number potentially differs between individual worms. An increased copy number among some worms may result in increased expression of SKN-B::GFP and ultimately increase neurone fluorescence independent of insulin signalling. Quantitative polymerase chain reaction (qPCR) can be used to indicate the degree of variation in transgene copy number between worms and so give insight into the source of neurone fluorescence intensity variation.

## 5. Conclusions

The AKT inhibitors AT13148 and MK2206 did not induce nuclear localisation of DAF-16 in *C. elegans,* though the exact reasons for this lack of an effect have yet to be determined. It was concluded that *C. elegans* is not a suitable model to test the effects of these particular drugs.

Knockout of SKN-1B appeared to result in reduced foraging behaviour, as a greater proportion of worms remained on the bacterial lawn in contrast to searching for a new food source. However, this difference between the *skn-1b(tm4241)* and N2 (WT) worms is small and more data should be collected before any confident conclusions can be stated.

SKN-1B expression is regulated by insulin signalling in the ASI neurones at 20°C and above, DAF-16 showing involvement of this at 20°C. It remains to be determined how this process operates and what function it has in worm physiology.
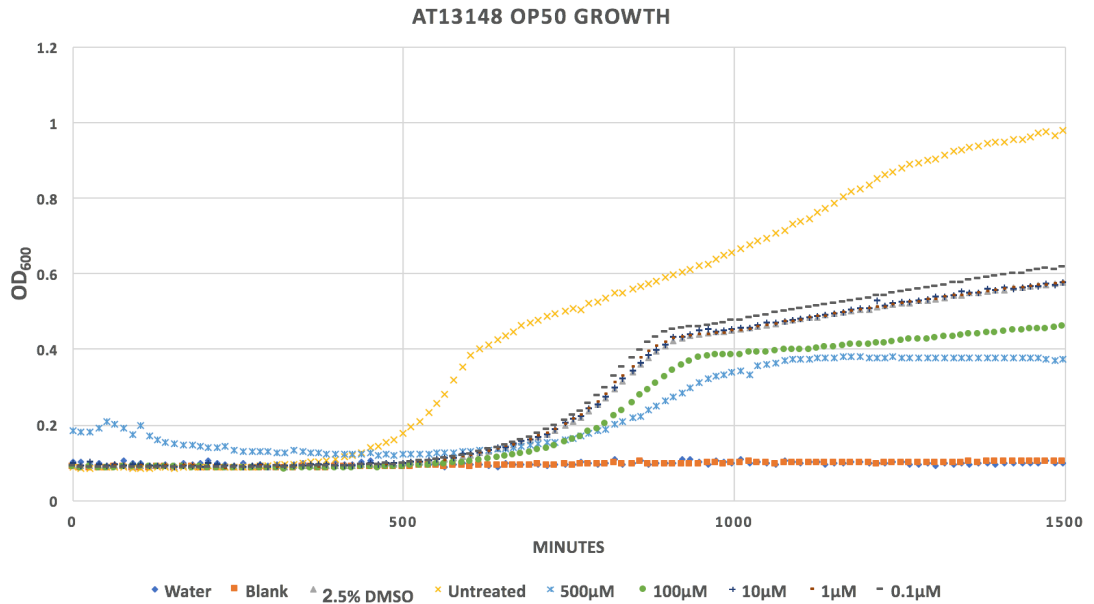
# 6. Appendix



*Figure 18 E. coli, OP50 strain, growth in the presence of various concentrations of AT13148. Data from three combined technical replicates of one biological replicate.*
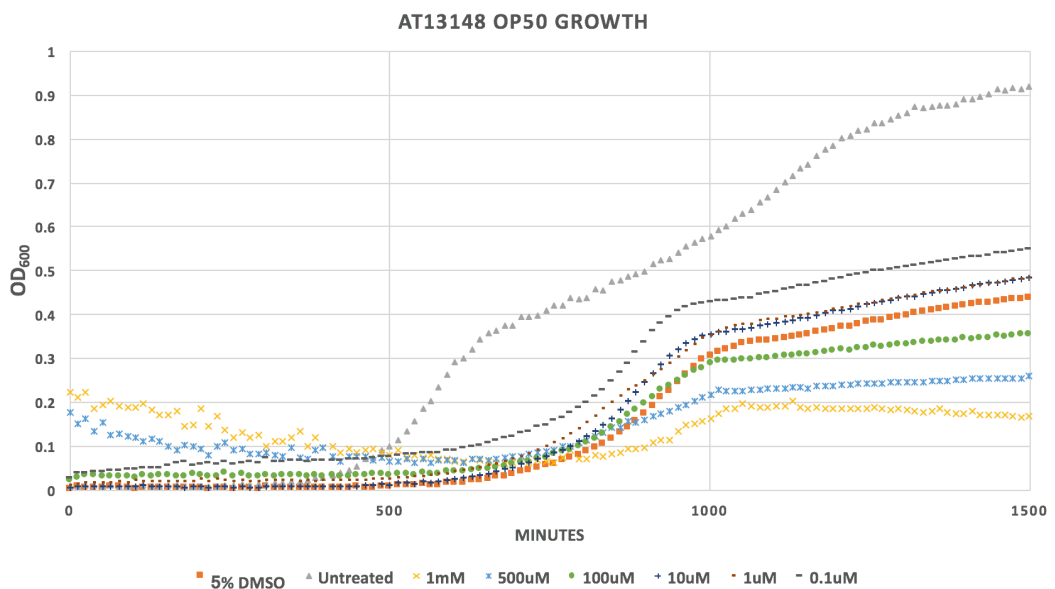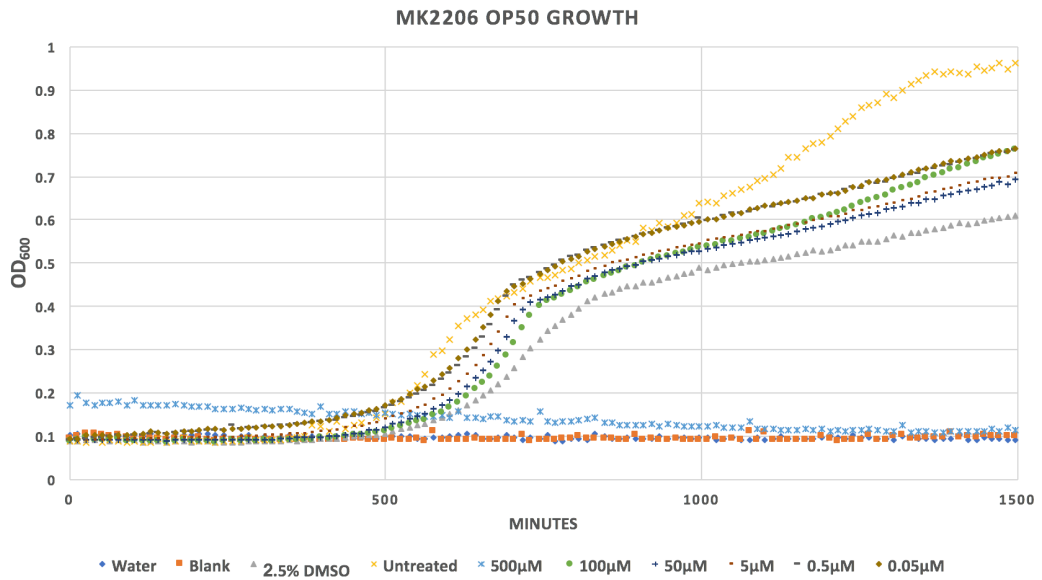


*Figure 19 E. coli, OP50 strain, growth in the presence of various concentrations of AT13148. Data from three combined technical replicates of one biological replicate.*

*Figure 20 E. coli, OP50 strain, growth in the presence of various concentrations of MK2206. Data from three combined technical replicates of one biological replicate.*
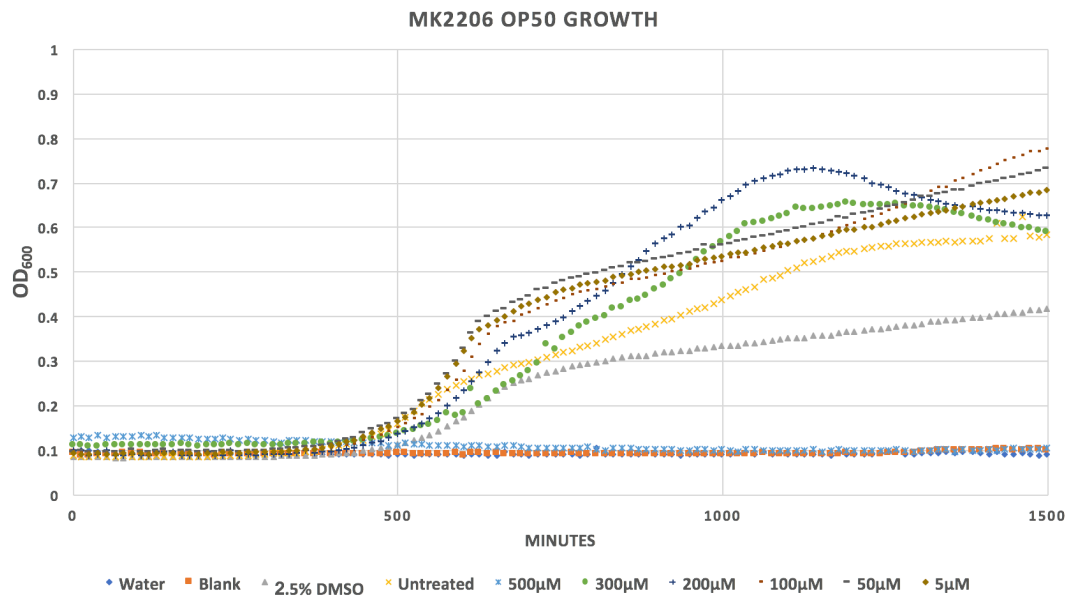


*Figure 21 E. coli, OP50 strain, growth in the presence of various concentrations of MK2206. Data from three combined technical replicates of one biological replicate.*

# 7. References

[1]     Kaletta, T. *et al.* Finding function in novel targets: C. elegans as a model organism. *Nat. Rev.* 5, 387–398 (2006).

[2]     Hodgkin, J. *et al.* Natural variation and copulatory plug formation in Caenorhabditis elegans. *Genetics* 146, 149–164 (1997).

[3]     Sulston, J. *et al.* Methods. *Cold Spring Harb. Monogr. Arch.* 17, (1988).

[4]     Madl, J. E. *et al.* Polyploids and sex determination in Caenorhabditis elegans. *Genetics* 93, 393–402 (1979).

[5]     Altun, Z. . *et al.* WormAtlas. Available at: http://www.wormatlas.org/. (Accessed: 22nd October 2016)

[6]     Baugh, L. R. To Grow or Not to Grow: Nutritional Control of Development During Caenorhabditis elegans L1 Arrest. *Genetics* 194, (2013).

[7]     Riddle, D. L. *et al.* Interacting genes in nematode dauer larva formation. *Nature* 290, 668–671 (1981).

[8]     Cassada, R. C. *et al.* The dauerlarva, a post-embryonic developmental variant of the nematode Caenorhabditis elegans. *Dev. Biol.* 46, 326–342 (1975).

[9]     Vowels, J. J. *et al.* Genetic analysis of chemosensory control of dauer formation in Caenorhabditis elegans. *Genetics* 130, 105–23 (1992).

[10]    Snutch, T. P. *et al.* Alterations in the pattern of gene expression following heat shock in the nematode Caenorhabditis elegans. *Can. J. Biochem. Cell Biol.* 61, 480–7 (1983).

[11]    Dalley, B. K. *et al.* Gene expression in the Caenorhabditis elegans dauer larva: Developmental regulation of Hsp90 and other genes. *Dev. Biol.* 151, 80–90 (1992).

[12]    Larsen, P. L. Aging and resistance to oxidative damage in Caenorhabditis elegans. *Proc. Natl. Acad. Sci. U. S. A.* 90, 8905–9 (1993).

[13]    Vanfleteren, J. R. *et al.* The gerontogenes age-1 and daf-2 determine metabolic rate potential in aging Caenorhabditis elegans. *FASEB J.* 9, 1355–61 (1995).

[14]    Broughton, S. *et al.* Insulin/IGF-like signalling, the central nervous system and aging. *Biochem. J.* 418, 1–12 (2009).

[15]    Cohen, E. *et al.* Temporal requirements of insulin/IGF-1 signaling for proteotoxicity protection. *Aging Cell* 9, 126–134 (2010).

[16]    Lin, K. *et al.* Regulation of the Caenorhabditis elegans longevity protein DAF-16 by insulin/IGF-1 and germline signaling. *Nat. Genet.* 28, 139–45 (2001).

[17]    Oh, S. W. *et al.* JNK regulates lifespan in Caenorhabditis elegans by modulating nuclear translocation of forkhead transcription factor/DAF-16. *Proc. Natl. Acad. Sci.* 102, 4494–4499 (2005).

[18]    Tao, L. *et al.* CAMKII and calcineurin regulate the lifespan of Caenorhabditis elegans through the FOXO transcription factor DAF-16. *Elife* 2, e00518 (2013).

[19]    Furuyama, T. *et al.* Identification of the differential distribution patterns of mRNAs and consensus binding sequences for mouse DAF-16 homologues. *Biochem. J.* 349, (2000).

[20]    Cahill, C. M. *et al.* Phosphatidylinositol 3-kinase signaling inhibits DAF-16 DNA binding and function via 14-3-3-dependent and 14-3-3-independent pathways. *J. Biol. Chem.* 276, 13402–10 (2001).

[21]    Tullet, J. M. A. *et al.* DAF-16/FoxO Directly Regulates an Atypical AMP-

Activated Protein Kinase Gamma Isoform to Mediate the Effects of Insulin/IGF-1 Signaling on Aging in Caenorhabditis elegans. *PLoS Genet.* 10, e1004109 (2014).

[22] Riesen, M. *et al.* MDL-1, a growth- and tumor-suppressor, slows aging and prevents germline hyperplasia and hypertrophy in C. elegans. *Aging (Albany. NY).* 6, 98–117 (2014).

[23] Murphy, C. . *et al.* Insulin/insulin-like growth factor signaling in C. elegans. *Wormbook* (2013). Available at: http://www.wormbook.org/chapters/www_insulingrowthsignal/insulingrowthsignal.html. (Accessed: 27th October 2016)

[24] Hirai, H. *et al.* MK-2206, an Allosteric Akt Inhibitor, Enhances Antitumor Efficacy by Standard Chemotherapeutic Agents or Molecular Targeted Drugs In vitro and In vivo. *Mol. Cancer Ther.* 9, 1956–1967 (2010).

[25] Yap, T. A. *et al.* AT13148 Is a Novel, Oral Multi-AGC Kinase Inhibitor with Potent Pharmacodynamic and Antitumor Activity. *Clin. Cancer Res.* 18, (2012).

[26] Shukla, S. *et al.* Apigenin: a promising molecule for cancer prevention. *Pharm. Res.* 27, 962–78 (2010).

[27] Ahn, D. H. *et al.* Results of an abbreviated phase-II study with the Akt Inhibitor MK-2206 in Patients with Advanced Biliary Cancer. *Sci. Rep.* 5, 12122 (2015).

[28] UniProtKB - Q17941 (AKT1_CAEEL). *UniProt* Available at: http://www.uniprot.org/uniprot/Q17941. (Accessed: 19th October 2016)

[29] Yang, J. *et al.* Crystal structure of an activated Akt/Protein Kinase B ternary complex with GSK3-peptide and AMP-PNP. *Nat. Struct. Biol.* 9, 940–944 (2002).

[30] Chen, X. *et al.* Using C. elegans to discover therapeutic compounds for ageing-associated neurodegenerative diseases. *Chem. Cent. J.* 9, 65 (2015).

[31] Zheng, S.-Q. *et al.* Drug absorption efficiency in Caenorhbditis elegans delivered by different methods. *PLoS One* 8, e56877 (2013).

[32] Partridge, F. A. *et al.* The C. elegans glycosyltransferase BUS-8 has two distinct and essential roles in epidermal morphogenesis. *Dev. Biol.* 317, 549–559 (2008).

[33] Gene: bus-8, Species: Caenorhabditis elegans - Caenorhabditis Genetics Center (CGC) - College of Biological Sciences. Available at: https://cgc.umn.edu/gene/243413. (Accessed: 16th October 2017)

[34] Jonathan Hodgkin. CB6193 (strain) - WormBase : Nematode Information Resource. (2008). Available at: http://www.wormbase.org/species/c_elegans/strain/CB6193#02--10.

[35] Blackwell, T. K. *et al.* SKN-1/Nrf, stress responses, and aging in Caenorhabditis elegans. *Free Radic. Biol. Med.* 88, 290–301 (2015).

[36] An, J. H. *et al.* SKN-1 links C. elegans mesendodermal specification to a conserved oxidative stress response. *Genes Dev.* 17, 1882–93 (2003).

[37] Walker, A. K. *et al.* A conserved transcription motif suggesting functional parallels between Caenorhabditis elegans SKN-1 and Cap'n'Collar-related basic leucine zipper proteins. *J. Biol. Chem.* 275, 22166–71 (2000).

[38] Blackwell, T. K. *et al.* Formation of a monomeric DNA binding domain by Skn-

1 bZIP and homeodomain elements. *Science* 266, 621–8 (1994).

[39]    Liochev, S. I. Reactive oxygen species and the free radical theory of aging. *Free Radic. Biol. Med.* 60, 1–4 (2013).

[40]    Tullet, J. M. A. *et al.* Direct inhibition of the longevity-promoting factor SKN-1 by insulin-like signaling in C. elegans. *Cell* 132, 1025–38 (2008).

[41]    Tullet, J. M. A. *et al.* The SKN-1/Nrf2 transcription factor can protect against oxidative stress and increase lifespan in *C. elegans* by distinct mechanisms. *Aging Cell* (2017). doi:10.1111/acel.12627

[42]    Bishop, N. a *et al.* Two neurons mediate diet-restriction-induced longevity in C. elegans. *Nature* 447, 545–9 (2007).

[43]    Katewa, S. D. *et al.* Dietary restriction and aging, 2009. *Aging Cell* 9, 105–12 (2010).

[44]    Avery, L. The genetics of feeding in Caenorhabditis elegans. *Genetics* 133, 897–917 (1993).

[45]    Remmert, M. *et al.* HHblits: lightning-fast iterative protein sequence searching by HMM-HMM alignment. *Nat. Methods* 9, 173–175 (2011).

[46]    Jones, D. T. Protein secondary structure prediction based on position-specific scoring matrices 1 1Edited by G. Von Heijne. *J. Mol. Biol.* 292, 195–202 (1999).

[47]    Jefferys, B. R. *et al.* Protein Folding Requires Crowd Control in a Simulated Cell. *J. Mol. Biol.* 397, 1329–1338 (2010).

[48]    Rotkiewicz, P. *et al.* Fast procedure for reconstruction of full-atom protein models from reduced representations. *J. Comput. Chem.* 29, 1460–1465 (2008).

[49]    Kelley, L. A. *et al.* The Phyre2 web portal for protein modeling, prediction and analysis. *Nat. Protoc.* 10, 845–858 (2015).

[50]    Rehan, M. *et al.* Computational insights into the inhibitory mechanism of human AKT1 by an orally active inhibitor, MK-2206. *PLoS One* 9, e109705 (2014).

[51]    Galvao, J. *et al.* Unexpected low-dose toxicity of the universal solvent DMSO. *FASEB J.* 28, 1317–30 (2014).

[52]    Cabreiro, F. *et al.* Metformin Retards Aging in C. elegans by Altering Microbial Folate and Methionine Metabolism. *Cell* 153, 228–239 (2013).

[53]    Scott, T. A. *et al.* Host-Microbe Co-metabolism Dictates Cancer Drug Efficacy in C. elegans. *Cell* 169, 442–456.e18 (2017).

[54]    Abada, E. A. *et al.* C. elegans behavior of preference choice on bacterial food. *Mol. Cells* 28, 209–213 (2009).

[55]    Shtonda, B. B. *et al.* Dietary choice behavior in Caenorhabditis elegans. *J. Exp. Biol.* 209, 89 (2006).

[56]    Sánchez-Blanco, A. *et al.* Dietary and microbiome factors determine longevity in Caenorhabditis elegans. *Aging (Albany NY)* 8, 1513 (2016).

[57]    Lee, D. *et al.* Effects of nutritional components on aging. *Aging Cell* 14, 8 (2015).

[58]    Gems, D. *et al.* Two pleiotropic classes of daf-2 mutation affect larval arrest, adult behavior, reproduction and longevity in Caenorhabditis elegans. *Genetics* 150, 129–55 (1998).

[59]    Hertweck, M. *et al.* C. elegans SGK-1 Is the Critical Component in the

Akt/PKB Kinase Complex to Control Stress Response and Life Span. *Dev. Cell* 6, 577–588 (2004).

[60]   Perrin, C. *et al.* Nickel promotes biofilm formation by Escherichia coli K-12 strains that produce curli. *Appl. Environ. Microbiol.* 75, 1723–33 (2009).

[61]   Wilson, M. A. *et al.* Skn-1 is required for interneuron sensory integration and foraging behavior in Caenorhabditis elegans. *PLoS One* 12, 1–14 (2017).

[62]   Dhondt, I. *et al.* FOXO/DAF-16 Activation Slows Down Turnover of the Majority of Proteins in C. elegans. *Cell Rep.* 16, 3028–3040 (2016).

[63]   Cáceres, I. de C. *et al.* Laterally Orienting C. elegans Using Geometry at Microscale for High-Throughput Visual Screens in Neurodegeneration and Neuronal Development Studies. *PLoS One* 7, e35037 (2012).